



RESEARCH

Early warning signals of complex critical transitions in deterministic dynamics

Kyra Evers · Denny Borsboom · Eiko I. Fried · Fred Hasselman · Lourens Waldorp

Received: 8 February 2024 / Accepted: 13 July 2024 / Published online: 5 August 2024
© The Author(s) 2024

Abstract Early Warning Signals (EWS) have generated much excitement for their potential to anticipate transitions in various systems, ranging from climate change in ecology to disease staging in medicine. EWS hold particular promise for bifurcations, a transition mechanism in which a smooth, gradual change in a control parameter of the system results in a rapid change in system dynamics. The predominant reason to expect EWS is because many bifurcations are preceded by *Critical Slowing Down* (CSD): if assuming the system is subject to continuous, small, Gaussian noise, the system is slower to recover from perturbations

Supplementary Information The online version contains supplementary material available at <https://doi.org/10.1007/s11071-024-10023-0>.

K. Evers (✉) · D. Borsboom · L. Waldorp
Psychological Methods Group, University of Amsterdam, Amsterdam, The Netherlands
e-mail: kyra.c.evers@gmail.com

D. Borsboom
e-mail: dennyborsboom@gmail.com

L. Waldorp
e-mail: ljwaldorp@gmail.com

E. I. Fried
Department of Psychology, Leiden University, Leiden, The Netherlands
e-mail: eiko.fried@gmail.com

F. Hasselman
Behavioural Science Institute, Radboud University, Nijmegen, The Netherlands
e-mail: fred.hasselmann@ru.nl

closer to the transition. However, this focus on warning signs generated by stochasticity has overshadowed warning signs which may already be found in *deterministic* dynamics. This is especially true for higher-dimensional systems, where more complex attractors with intrinsic dynamics such as oscillations not only become possible—they are increasingly more likely. The present study focuses on univariate and multivariate EWS in deterministic dynamics to anticipate complex critical transitions, including the period-doubling cascade to chaos, chaos-chaos transitions, and the extinction of a chaotic attractor. In a four-dimensional continuous-time Lotka–Volterra model, EWS perform well for most bifurcations, even with lower data quality. The present study highlights three reasons why EWS may still work in the absence of CSD: changing attractor morphology (size, shape, and location in phase space), shifting power spectra (amplitude and frequency), and chaotic transitional characteristics (density across attractor). More complex attractors call for different warning detection methods to utilise warning signs already contained within purely deterministic dynamics.

Keywords Early Warning Signals · Global bifurcation · Chaotic bifurcation · Lotka–Volterra model · Critical transition · Regime shift

1 Introduction

All systems exhibit temporal dynamics. These changes across time may be the oscillations of a pendulum, the rhythmic beating of a heart, or the fluctuations in financial markets. Bigger system changes, such as the extinction of a species or the onset of depression, may be called *regime shifts*: large, qualitative differences in system structure and behaviour [1]. Some regime shifts may be anticipated using Early Warning Signals (EWS), which are statistical indicators of an upcoming transition. In the case of undesirable shifts such as a disease outbreak, knowing if and when a shift is coming would be profoundly useful, enabling one to prepare, mitigate or even avoid the shift altogether. EWS are for example expected for bifurcation-induced transitions, in which small, continuous changes in system parameters result in sudden, qualitative changes in behaviour [2,3]. In this paper, we focus on anticipating switches between complex attractors, such as limit cycles and chaotic attractors. As the extent to which EWS can be expected for complex bifurcations remains unclear, we demonstrate how typical characteristics of complex attractors might underlie the warning signs observed in *deterministic* dynamics.

A strong theoretical basis for EWS centres on the phenomenon of *Critical Slowing Down* (CSD): as the bifurcation point is approached, the current attractor loses its stability and the system is thus less quick to recover from perturbations [4–8]. Analytically, loss of stability is equivalent to the dominant eigenvalue of the linearised dynamics around the attractor approaching zero from below, which translates to a slower return rate to equilibrium [6]. Under the assumption of continuous state perturbations, this slower recovery rate means that perturbations have a more pronounced and persistent effect, which may be detected by rising variance and lag-1 autocorrelation, among other EWS. The hope for anticipating transitions using EWS thus centres primarily on CSD, which requires stochasticity in the form of continuous perturbations.

This theoretical narrative works nicely for critical transitions between fixed point attractors. For instance, most transitions are modelled using a pair of saddle-node bifurcations, which leads to the disappearance of a stable fixed point and the appearance of a new, distant fixed point which the system settles in. However, it is less clear what EWS to expect for transitions between attractors more complex than fixed points, such as limit

cycles and chaotic attractors. When moving to more realistic, higher-dimensional, non-linear models, more complex attractor types not only become possible—they are increasingly more likely. For instance, Random Matrix Theory indicates that both oscillatory [9] and chaotic dynamics [10, p. 1469] become more probable for increasing dimensionality [11]. Moreover, empirical systems from diverse fields have been speculated to contain complex attractors, such as in ecology [12,13], health care [14–17], neuroscience [18], as well as in mental health and psychotherapy [19–26]. Examples of critical transitions involving complex attractors include the birth of a limit cycle from a fixed point (Hopf bifurcation), period-doubling and period-halving bifurcations, chaos-chaos and periodic-chaotic transitions. Such complex critical transitions not only include local bifurcations, but also *global* bifurcations. Local bifurcations correspond to topological changes concentrated in a small region around fixed points, which are well described by an analytical analysis [27,28], [29, p. 197]. Conversely, global bifurcations result in larger altered regions of phase space, involving the collision between invariant sets with each other or with equilibria [30]. They are *always* catastrophic [12], and involve attractors covering larger regions of phase space or distant attractors, as for instance a homoclinic connection between two fixed points.

In the case of complex and chaotic attractors, it is unclear whether EWS based on CSD can be expected. Analytically, chaotic and global bifurcations are not expected to be preceded by generic EWS. Chaotic attractors are inherently locally unstable, such that a global gradual loss of stability is not reflected locally. A typical local stability analysis of fixed points has little relevance for complex critical transitions, which may have non-smooth, fractal potentials or involve switches between distant attractors (global bifurcations) [31]. Fractals, such as the famous Mandelbrot or Cantor set, are “complex geometric shapes with fine structure at arbitrarily small scales” [32, p. 398], consisting of “an infinite complex of surfaces” [33, p. 140]. Rather than the exception, non-smooth potentials are the norm in the case of multiple attractors [31, p. 467], and are not well approximated by a linearization. As such, CSD and its typical reflection in EWS are not expected to occur [31].

Simulation studies—though sparse—have shown mixed results on EWS for complex and chaotic bifurcations. Using several higher-dimensional models in both

continuous and discrete time, Hastings and Wysham [31] found no clear, reliable change in variance and skew in anticipation of several chaotic switches. In contrast, using a similar model as Hastings and Wysham, Carpenter and Brock [34] *did* find strong EWS, though focusing on spatial patterns of the entire system and not on individual spatial patches. Similarly, Dakos et al.'s [35] study of a one-dimensional discrete Ricker model with intrinsic noise observed changes in lag-1 autocorrelation and coefficient of variation (μ/σ) in anticipation of period-doubling as well as the onset of chaos [35]. The warnings were not peaks, but gradual increases proportional to a gradually changing parameter. Moreover, several studies have found evidence for EWS of global bifurcations [36–38].

Given the ambiguity on whether to expect EWS for complex bifurcations, the goal of the current paper is to build towards a step-wise understanding by starting with EWS harboured in *deterministic* dynamics. When studying fixed-point bifurcations, deterministic dynamics are hardly interesting, as only the location of the fixed point may change. In contrast, complex attractors allow for a much wider array of warning signals, as they are characterised by not only their location in phase space, but also their size and shape, differences in density and speed along the attractor, and sometimes switches between smaller attractors contained within the larger attractor. Even in the absence of stochasticity, properties of complex attractors that gradually change along with a smoothly changing bifurcation parameter are expected to show EWS.

In the present study, we aim to clarify this uncertain picture by testing the performance of a broad range of EWS in a multitude of complex critical transitions. In a continuous Generalised Lotka–Volterra model of four dimensions, the transitions studied include fixed point bifurcations such as the Hopf and saddle-node bifurcation, limit cycles bifurcations such as period-doubling and period-halving sequences, and chaotic bifurcations, such as the subduction, the interior crisis, and the boundary crisis (see Fig. 1). Taking a simple yet fundamental approach, we investigate EWS contained in *deterministic* dynamics without any stochasticity. The intrinsic dynamics of complex attractors already yield fluctuating EWS in null models, in which no parameter is changing. This necessitates incorporating both sensitivity and specificity into the performance of EWS, which is summarised using the Area Under the Curve (AUC) of the receiver operating characteristic

(ROC) curve of each measure's false positive vs. true positive rate. Finally, we test the dependency of EWS on data quality (sampling frequency and measurement noise). Our findings argue for the lack of a universal EWS signature and the many warning signs which may already be present in deterministic dynamics.

2 Methods

2.1 The Generalised Lotka–Volterra model (GLV)

To examine the utility of EWS in anticipating various critical transitions, we choose a model that is able to display a rich array of complex attractors: the Generalised Lotka–Volterra (GLV) Model. Based on the logistic growth model, the range and stability of the behaviour of the GLV has been extensively analysed [11, 39–41], and is used to model mutualistic and competitive multidimensional systems in ecology [42, 43], cognitive science [44], economics [45, 46], and more recently, emotion dynamics [47, 48].

The GLV describes a system of N species competing for limited resources, and how they interact and evolve over time. The model includes a growth or death rate r_i as well as community matrix encoding interspecies dynamics C ,

$$\frac{dx_i}{dt} = r_i x_i \left(1 - \sum_{j=1}^N C_{ij} x_j \right) \tag{1}$$

C_{ij} denotes the effect of an increase in species j on species i , or equivalently, the receiving effect of species i from species j [49]. Extending the simple two-species predator–prey model with only competitive interactions, the GLV can display three types of interactions: competitive ($C_{ij} > 0$ and $C_{ji} > 0$) (note the minus sign in Eq. 1), mutualistic ($C_{ij} < 0$ and $C_{ji} < 0$), or predator–prey ($C_{ij} > 0$ and $C_{ji} < 0$, or $C_{ij} < 0$ and $C_{ji} > 0$).

Manipulating the connectivity matrix C in a specific way results in a well-studied sequence of regimes [42]: the onset of oscillations with increasing amplitude in a Hopf bifurcation, with increasingly intricate oscillations created by a period-doubling cascade to chaos, which is interrupted by intermittent periodic windows, ending in a boundary crisis in which the chaotic attractor is extinguished, after which the system settles into

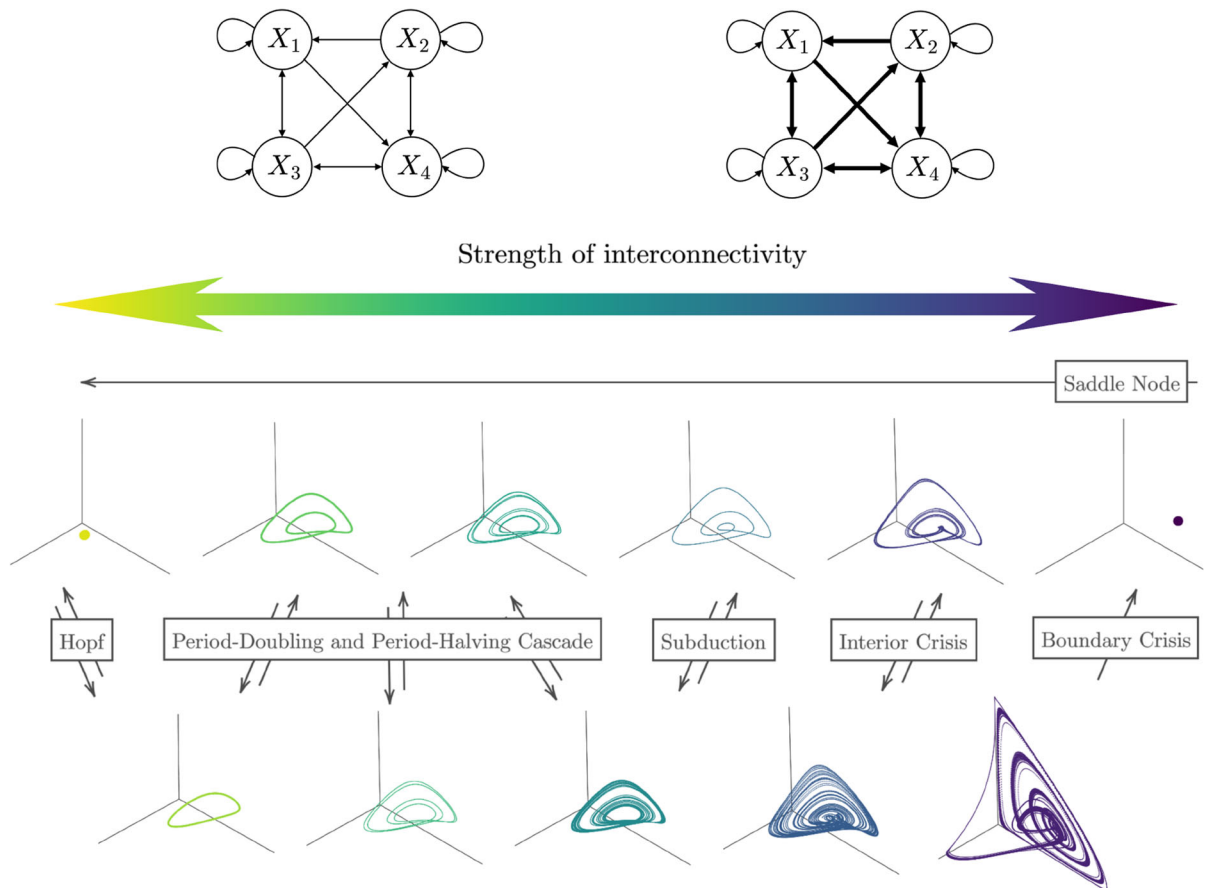


Fig. 1 Overview of the Generalised Lotka–Volterra (GLV) model and included bifurcations. The system consists of four variables (top panel), which are *interconnected* through \mathbf{C} and *intraconnected* through \mathbf{r} (see Sect. 2.1). The strength s of the interconnectivity acts as the control parameter of the system, where higher s results in greater competition for resources between variables, concurrent with a diminished growth rate (since \mathbf{r} remains fixed) of each variable. Bifurcation sequences were generated both by increasing and decreasing s (double-headed arrow), as shown in the three-dimensional phase space landscapes of $[X_3, X_2, X_1]$ (bottom panel). Increasing s (arrows

pointing to the right) results in a typical sequence of bifurcations, involving the birth of a limit cycle from a fixed point (Hopf bifurcation), increasingly intricate limit cycles through period-doubling bifurcations (period-2 to period-4, period-4 to period-8, period-8 to period-16) culminating in chaos (mixed-periodic to chaotic) which switches back to periodic behaviour (subduction). By increasing s further, a transition between chaotic attractors takes place to a more densely filled attractor (interior crisis), finishing with the extinction of the chaotic attractor (boundary crisis). Decreasing s (arrows pointing to the left) results in a similar sequence of bifurcations, though now from the other direction

a fixed point. Though a specific set of parameters is required to achieve this sequence of behaviours, these critical transitions are quite generic and occur widely across alternative realisations of the GLV and many other dynamical systems [12, 50–52], making them of general interest to non-linear and chaotic systems.

Specifically, this sequence of dynamical regimes may be generated by fixing

$$\mathbf{r} = \begin{bmatrix} 1 \\ 0.72 \\ 1.53 \\ 1.27 \end{bmatrix} \quad \mathbf{C} = \begin{bmatrix} 1 & 1.09 & 1.52 & 0 \\ 0 & 1 & 0.44 & 1.36 \\ 2.33 & 0 & 1 & 0.47 \\ 1.21 & 0.51 & 0.35 & 1 \end{bmatrix}$$

and multiplying the off-diagonal elements of \mathbf{C} with a single control parameter s , as discovered by [39]. If $s = 0$, the system is completely decoupled. Increasing the control parameter s results in increasing inter-

Table 1 Bifurcations studied

Bifurcation	Class	Behaviour	CSD	Direction s
Saddle-node	Dangerous	Node to node	✓[5]	Backward
Hopf	Safe	Node to periodic	✓[9,53–55]	Both
Period-doubling	Safe	Periodic to periodic	✓[56,57]	Both
Period-doubling cascade	Safe [58]	Periodic to chaotic	✓[57]	Both
Subduction	Explosive	Periodic to chaotic	✓[27]	Both
Interior crisis	Explosive	Chaotic to chaotic	✗[27,59]	Both
Boundary crisis	Dangerous	Chaotic to node	✗[27,59]	Forward

Each bifurcation is categorised as safe, explosive, or dangerous using Thompson and Sieber’s [27] classification scheme (see Table 2). Behaviour indicates the system’s regime before and after the bifurcation point, which may be preceded by Critical Slowing Down (CSD). Most bifurcations were studied with increasing s (direction forward) and decreasing s (direction backward)

Table 2 Properties of bifurcation classes (safe, explosive, dangerous) as indicated in Table 1

Property	Definition	Safe	Explosive	Dangerous
Catastrophic	The old attractor suddenly disappears, and the new attractor appears in a non-smooth, non-continuous way	✗	✓	✓
Sudden jump to a new attractor	A sudden jump to another attractor and/or an enlargement of the attracting set	✗	✗	✓
Determinate	A deterministic outcome even under small noise, not dependent on the global typology of phase space	✓	✓	✗
Hysteresis	The regime switch cannot be reversed by returning to the same value of the control parameter	✗	✗	✓
Basin change	New attractor collides with the residual basin boundary	✗	✗	✓
Intermittency	Switches between the old and new attractor	✗	✓	✗

These properties help to understand the variability in the (ir)reversibility and underlying phase space changes among bifurcation types, and may also inform what EWS to expect

species competition (as the species are purely competitive) while holding the growth rate r_i constant (see Fig. 1, top panel). As transitions are induced by manipulating only one control parameter, all resulting bifurcations are of co-dimension one [32, p. 70]. Importantly, **C** is asymmetrical, which allows the system to occupy a large range of complex attractors.

2.2 Selected bifurcations

The simulation includes nine bifurcations for which it was possible to generate both directions of the transition for seven bifurcations, resulting in a total of sixteen transitions (Table 1, Fig. 1, Supplementary Table

S2). Following Thompson and Sieber’s [27,60] classification, the transitions consist of safe, explosive, and dangerous bifurcations. This classification helps to understand the variation among bifurcation types, their (ir)reversibility, and their underlying phase space changes. In addition, these classes inform predictions of EWS, as for instance safe bifurcations are non-catastrophic, meaning they develop in a smooth, continuous fashion (Table 2).

There are four classical ways in which chaotic attractors can be created—or destroyed, if the process is reversed. The four *routes to chaos* are the period-doubling cascade (a series of period-doubling bifurcations gives birth to a chaotic attractor), quasi-

periodicity (a limit cycle develops into a torus displaying quasi-periodic motion, which then develops into a chaotic attractor [52, Ch. 6]), intermittency (periodic motion is intermittently interrupted by chaotic bursts, before finally settling on the chaotic attractor), and the crisis route (transient chaos transforms into a chaotic attractor) [17, 61]. Naturally, steps in these routes may themselves serve as warnings of oncoming chaos.

Below, we briefly describe each bifurcation type.

2.2.1 Saddle-node bifurcation: the disappearance of a stable fixed point

A *saddle-node bifurcation* (also called a tangent bifurcation, or fold bifurcation in discrete-time systems) is a mechanism through which fixed points are created and destroyed. In the typical case used to model critical transitions, a pair of saddle-node bifurcations connects two stable branches and one unstable branch. The system starts out on the first stable branch, representing the slowly changing fixed point coordinates as the control parameter changes. At the first saddle-node bifurcation s_{crit}^1 , the stable fixed point collides with an unstable fixed point, annihilating both. The system jumps to the far-removed second stable branch. To return to the first stable branch, the control parameter would have to be decreased not to s_{crit}^1 but to the much lower second saddle-node bifurcation point s_{crit}^2 . At s_{crit}^2 , the second stable branch collides with an unstable fixed point, again leading to the destruction of both, leading the system to jump back to the first stable branch. A saddle-node bifurcation is a local phenomenon which in any continuous system is preceded by CSD [5].

2.2.2 Supercritical Hopf bifurcation: the birth of a limit cycle

A *Hopf bifurcation* (Neimark–Sacker bifurcation in discrete-time systems) is a local bifurcation which gives birth to a limit cycle. Just like its more studied siblings the saddle-node, pitchfork, and transcritical bifurcation, the Hopf is a *zero-eigenvalue bifurcation* (in which the dominant eigenvalue of the linearised dynamics around the attractor reaches zero at the bifurcation point). Unlike the other zero-eigenvalue bifurcations, the Hopf bifurcation occurs only for systems of dimensionality two or higher and involves oscillatory dynamics due to the imaginary part of the associated eigenvalues. In a supercritical Hopf bifurcation,

a pair of complex conjugate eigenvalues (having both a real and imaginary part, $\lambda = a \pm bi$) crosses the imaginary axis, gaining a positive real part. As such, oscillations are no longer dampened, and the system transitions from a stable spiral to a limit cycle.

2.2.3 Period-doubling and period-halving: increasingly and decreasingly intricate limit cycles

Period-doubling and period-halving bifurcations are mechanisms through which a limit cycle can become more intricate or more simplistic, respectively. In a supercritical period-doubling bifurcation (also called a flip bifurcation in discrete-time systems), a stable periodic cycle bifurcates into a new stable periodic cycle of double its period. Whereas for $s < s_{\text{crit}}$, the period of the cycle (i.e. the length of one full oscillation) was T , such that $x(t + T) = x(t)$, after the period-doubling bifurcation, it has doubled to $2T$. In this way, the limit cycle becomes more intricate, involving a more complex pattern that is still perfectly periodic.

A sequence of such period-doubling bifurcations is a well-known route to chaos, called an infinite period-doubling cascade [42, 62]. Such a sequence would typically create limit cycles of period 2, 4, 8, 16, and so on. The time between these bifurcations follows a universal pattern as discovered by Feigenbaum, where each n th bifurcation point s_{crit}^n occurs in quicker succession, as given by the Feigenbaum constant. Naturally, we may also observe the inverse: a period-halving cascade, consisting of successive period-halving bifurcations leading to order. A similar reverse cascade creates limit cycles of period 16, 8, 4, 2, and 1, returning to a stable fixed point in a backwards Hopf bifurcation.

Period doubling bifurcations in the context of EWS have been studied by [9, 63–66], with sparse literature on EWS for period-halving bifurcations [65]. Classical EWS such as rising variance, lag-1 autocorrelation and spectral power are observed in period-doubling sequences in discrete time [9, 35].

2.2.4 Crises: dramatic (dis)appearance of a chaotic attractor

Crises are bifurcations leading to the destruction or creation of a chaotic attractor. Unlike the previous three bifurcations discussed, crises are *global* events, and are always *catastrophic*. As such, they involve larger

invariant sets (i.e. not only fixed points but attractors spread out over larger regions of phase space) and discontinuous, sudden switches between attractors. Crises occur when a chaotic attractor collides with an unstable node or periodic cycle [67], leading to its extinction or expansion, or in reverse, its birth or reduction. By definition, a chaotic attractor is locally unstable but globally stable, where the latter is lost at the crisis point.

The two most well-known crises are the *interior crisis* and the exterior or *boundary crisis*. In an interior crisis, a chaotic attractor collides with an unstable cycle and subsumes the basin of another chaotic attractor [12], leading to a sudden increase in the size and change in the shape of the chaotic attractor [67]. In a boundary crisis, a chaotic attractor collides with an unstable cycle which is on the boundary of the attracting basin, leading to the disappearance of the chaotic attractor. Its basin of attraction does not gradually shrink to zero as in a saddle-node bifurcation, but is destroyed suddenly and completely [27].

2.2.5 Subduction: sudden shift between periodic and chaotic behaviour

In a *subduction*, a chaotic attractor suddenly converts to a periodic attractor or vice versa. Subductions underlie the familiar islands of periodicity interspersed between chaotic regions found in many bifurcation diagrams [51, p. 4]. A subduction is a type of saddle-node bifurcation (also called tangent bifurcation) in which a stable and unstable orbit are created as a chaotic attractor collides with a stable periodic orbit [51, p. 94], [60,67,68]. A subduction is thus not a crisis, but a local bifurcation that occurs within a global structure [60,67]. The chaotic attractor is replaced by the new periodic orbit, but continues to exist throughout the periodic window as a non-attracting chaotic set. The end of the periodic window often occurs due to the collision of the non-attracting chaotic set with another chaotic attractor. This bifurcation results in the replacement of the periodic orbit with the new chaotic attractor [51, p. 94].

2.3 Selected early warning signals

An overview of the studied EWS may be found in Table 3. As the EWS signature of complex critical transitions is largely unexplored, we aimed for a comprehensive overview.

Table 3 Overview of selected early warning signals

Class	Early warning signals
Generic univariate	Mean [69]
	Variance [70]
	Coefficient of variation [70]
	Skewness [71]
	Kurtosis [3]
Multivariate	Lag-1 autocorrelation [72]
	Mean absolute cross-correlation [73]
	Largest eigenvalue of the covariance matrix [74]
	Spatial variance [75]
	Spatial skewness [75]
Spectral univariate	Spatial kurtosis [75]
	Maximum spectral density [9]
	Spectral exponent [76,77]
	Spectral ratio [3]

Table 4 Overview of simulation parameters

Parameter	Setting	Meaning
N_{sim}	25	Number of simulation models
T	1000	Number of time steps to simulate per step s_i in the bifurcation parameter
Δ_t	.01	Euler integration time step
Baseline N_s	100	Number of steps in s in baseline period
Transition N_s	100	Number of steps in s in transition period
N_{noise}	10	Number of noise simulations per simulation model
f_s	[10, 1, .1]	Downsampling frequency
σ_{obs}	[0.0001, .02, .04]	Observational noise intensity

2.4 Simulation and analysis

We here outline an overview of the set-up to generate time series for each bifurcation type, compute EWS, and summarise the performance of each EWS per bifur-

cation type. An overview of the simulation parameters can be found in Table 4. For details and variations on the implementation per bifurcation type, please see the Supplementary Materials, section S1.1.2. An algorithm summarizing the procedure may be found in the Supplementary Materials (section S1.1.2, algorithm 2).

2.4.1 Generating time series of critical transitions

For each bifurcation type, our objective is to simulate multiple realisations starting from different initial conditions. The need for multiple realisations of the same bifurcation may seem strange in a deterministic system. This is indeed unnecessary in the case of systems where the entire control parameter range is *monostable*, meaning that only a single attractor exists whose basin of attraction occupies the entire state space; all initial conditions converge to the same attractor. In contrast, in *multistable* regions, differences in initial conditions *do* result in different bifurcation sequences (see Supplementary Figure S5). Particularly in the case of fractal basin boundaries [32, p. 447], [51, p. 147], [78–80], the most minor difference in initial conditions can make the system converge to a different attractor. Fractal basin boundaries are common to many systems and attractors (e.g. Duffing oscillator, forced damped pendulum), and especially for chaotic attractors, where a difference in initial conditions also results in a different density along the attractor. Because of this dependence on initial conditions, we use multiple realisations for each bifurcation type in order to make more general conclusions about the predictability of each bifurcation type.

As the range of bifurcations possible in the GLV is vast (see Fig. 2), we first forced the GLV through nearly the entire parameter range s (see Table S2 for all ranges s used) in order to identify parameter regions containing bifurcations of interest. Bifurcation diagrams were numerically obtained by finding the peaks and troughs (i.e. local minima and maxima) of the time series using the R package *pracma* [81]. Note that transients are included in the diagram to show the full transitional process, meaning that the entire time series was used without discarding a burn-in period. To find the parameter regions corresponding to the bifurcations of interest, we used a custom regime boundary detection algorithm (see Supplementary Materials, section S1.1.1). This numerical algorithm finds the control parameter values which delimit each regime, as well as the state variable values which may be used as initial condi-

tions. Using these regime boundaries and initial conditions (the initial condition x_0 and bifurcation parameter value s_1 halfway across the first regime, as well as the starting bifurcation parameter value s_2 of the second regime), we may generate both a transition and a null model for each realisation. The transition and null model start from an identical initial condition and control parameter value, but whereas the control parameter stays constant in the null model, the transition model is forced through a bifurcation by changing the control parameter in a step-wise fashion. The null model therefore shows the fluctuations that are expected in EWS in the first regime.

Per bifurcation type, $N_{\text{sim}} = 25$ realisations (i.e. 25 transition and 25 null models) were created. The control parameter was changed in steps, where for each step in N_s , a time series was generated with $T = 1000$ and time step $\Delta_t = .01$ and (i.e. length 100,000) using Runge–Kutta (4th order) integration available in the *ode* function from the *deSolve* package [82] (exceptions to these settings depending on bifurcation type may be found in the Supplementary Materials, section S1.1.2). In each model, the control parameter was kept constant at s_1 for $N_s = 200$ steps, followed by a transitional period with $s \in [s_1, s_2]$ changed in $N_s = 100$ equally-sized steps (for null models, s was kept at s_1), ending with a post-bifurcation period with s fixed at s_2 for $N_s = 100$ (for null models, s was kept at s_1).

Bifurcation types differ in the size of the parameter regions at which the first and second regime are found. For example, though the Hopf bifurcation is preceded by a fixed point regime found in $s \approx [.6, .83]$, the interior crisis (merging) is preceded by a small chaotic attractor contained in the narrow range $s \approx [1.011, 1.0125]$ (see Fig. 2). In order to ensure that EWS were comparable across bifurcation types, the *number* of steps N_s in the control parameter was the same across bifurcation types, but the *size* of each step Δ_s differed.

Importantly, the present study includes warning signals contained within *transient* dynamics. Transient behaviour is not long-term stable and will die off as $t \rightarrow \infty$. However, it may be argued that many empirical systems operate on non-asymptotic timescales where transient behaviour is highly relevant [2]. Expectations of warning signs based on asymptotic dynamics may also be misleading, as a system is rarely observed for a sufficient amount of time in applied settings. We are therefore interested in warning signs in non-

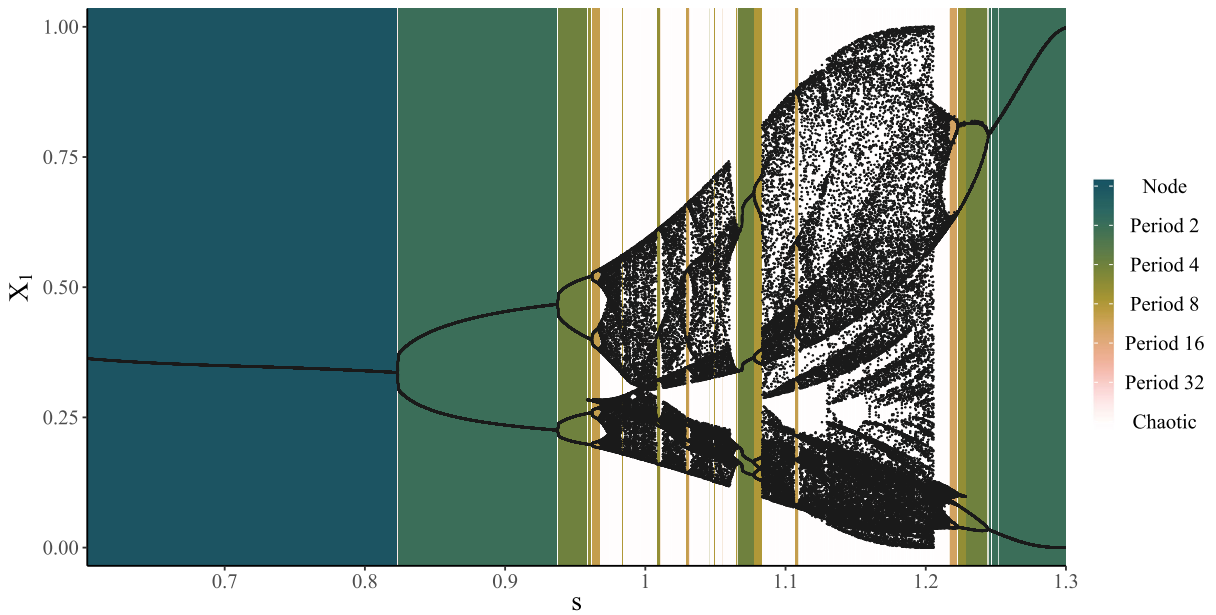


Fig. 2 Bifurcation diagram of the Generalised Lotka–Volterra model (only the first variable X_1), showing the sequence of transitions as the control parameter s is increased from $[.6, 1.3]$. For each step in s , the peaks and troughs (i.e. local minima and maxima) of the corresponding time series are shown as black points,

corresponding to each value of the bifurcation parameter s (x-axis). Coloured bars indicate the periodicity of the time series as found using our regime boundary detection algorithm, where white indicates chaotic or transitioning regimes

asymptotic dynamics. This has the important implication that even in the case of exactly the same control parameter sequence, slight variations in initial conditions can lead to differences in the control parameter value at which the transition is detected. As the transition is detected numerically, multiple realisations of the same bifurcation type with different initial conditions will not transition at the exact same control parameter value.

In order to ensure that the same amount of data was used for each realisation, as well as to check whether the simulation was successful, the regime boundary detection algorithm was also applied to the transition and null models. The realisation was retained only if the intended first regime and second regime were detected in the transition model, and only the first regime in the null model. The starting point of the second regime was then used as the transition point. The preceding $N_s = 100$ were used as the transitional period to detect EWS, and the $N_s = 100$ preceding the transitional period was used as the baseline period. As such, for the EWS analysis, each model was of length $N_s = 200$.

2.4.2 Computing early warning signals

EWS were computed for each step in s (i.e. non-overlapping windows). To assess the dependence of EWS performance on the quality of the dynamics, the time series were downsampled with frequencies $f_s \in [10, 1, .1]$ (i.e. retaining 10 samples per time unit, 1 sample per time unit, or 1 sample per 10 time units) and obscured by observational (additive) noise with intensities $\sigma_{\text{obs}} \in [0.0001, .02, .04]$, yielding 9 conditions. For each condition, 10 noise realisations were run, yielding 250 transition and null realisations per condition.

No preprocessing was applied to the time series, as it is not known which method best fits these wide-ranging bifurcation types, potentially removing warning signs in the process instead. For instance, detrending, deseasoning, filtering, interpolation, and data transformations can all impact which EWS are detected [77,83,84].

Note that transitions from a fixed point do not depend on the initial condition in the case of deterministic dynamics, such that only one realisation for the Hopf and saddle-node bifurcation was created. To still yield

the same number of noisy time series, 250 instead of 10 noise realisations are created. In case the time series had near zero variance (as is the case for fixed points with no observational noise), EWS were set to 0.

2.4.3 Performance measure: area under the curve (AUC)

Finally, the performance of EWS is summarised using receiver operating characteristic (ROC) curve, a standard approach which integrates the trade-off between sensitivity and specificity [85]. An ideal EWS maximises the number of true positives (resulting from transition models), and minimises false positives (resulting from null models). In brief, an EWS metric displays a warning sign if it falls outside the confidence band in the transition period. The confidence band or interval (CI) is constructed from the mean μ_{baseline} and standard deviation σ_{baseline} of the EWS metric in the baseline period using $\text{CI} = \mu_{\text{baseline}} + \sigma_{\text{baseline}} \cdot \sigma_{\text{crit}}$. By varying the critical threshold σ_{crit} , a ROC curve is constructed by counting the number of transition models with true positives and the number of null models with false positives for each σ_{crit} . To fully complete the ROC curve, we explored the entire range of σ_{crit} in steps of .01 for each model until $\text{TPR} = 0$ and $\text{FPR} = 0$, with a maximum of $\sigma_{\text{crit}} = 150$ (which is the case in rapid transitions with little baseline variance, such as the saddle-node bifurcation). The ROC curve traces the false positive rate (1 - specificity, i.e. $\text{FPR} = \frac{\text{FP}}{\text{FP} + \text{TN}}$) vs. true positive rate (sensitivity, i.e. $\text{TPR} = \frac{\text{TP}}{\text{TP} + \text{FN}}$).

Integrating the area under the curve (AUC) yields a performance measure which is independent of a single threshold, which would be arbitrary and not generalise to scenarios with different specificity to sensitivity trade-offs. A perfect measure corresponds to $\text{AUC} = 1$, where all thresholds yield only true and no false positives, whereas a measure with $\text{AUC} = .5$ is considered uninformative, where each threshold yields the same rate of false positives as true positives. Though cut-off values are field-specific and depend on the relative improvement in AUC compared to already existing measures, a starting point for classification identifies measures with $\text{AUC} \geq .9$ as excellent, $.8 \leq \text{AUC} < .9$ as good, $.7 \leq \text{AUC} < .8$ as fair, $.6 \leq \text{AUC} < .7$ as poor, and $.5 \leq \text{AUC} < .6$ as useless [86]. Given the high resolution of the AUC curve, simple trapezoidal integration was used to compute the area under

the curve using the function *trapz* from the R package *pracma* [81].

2.4.4 Timing and direction of EWS

The AUC is an incomplete performance measure, as it assesses the balance between sensitivity and specificity of EWS occurring at *any moment* before the transition. To gain more insight into the nature of each EWS, we looked at the direction and timing of warning signals given an optimised critical cut-off value σ_{crit} . The critical cut-off value σ_{crit} determines what signal counts as a warning signal. Higher σ_{crit} results in not only fewer but also *later* warning signals, as the signal has to be stronger to pass the cut-off value and be recognized as a warning. Conversely, lower σ_{crit} yields greater sensitivity but reduced specificity, with more as well as earlier warning signals. As it is crucial whether warning signals are on time in any practical setting, a single cut-off value is needed, for which we used Youden's *J* statistic [87]: $J = \text{Sensitivity} + \text{Specificity} - 1$, or rewritten as $J = \text{TPR} - \text{FPR}$. It finds the cut-off value for which the sensitivity and specificity are highest, weighing them as equally important.

Setting a single critical cut-off value σ_{crit} also allows us to see in which *direction* the warning is: Is the EWS *increasing* or a *decreasing* as compared to baseline? To summarise the timing and direction of EWS across simulations, we found the σ_{crit} that corresponded to the maximum *J* statistic for each combination of bifurcation type, metric, downsampling frequency f_s and observational noise intensity σ_{obs} . We then extracted the first warning signal that resulted from this optimal cut-off value σ_{crit}^* from all simulations and noise iterations of transition models. To aggregate across different data quality conditions (downsampling frequency f_s and observational noise intensity σ_{obs}), we computed the median time of the warning signal as well as the percentage of warning signals showing an increase as compared to baseline (i.e. the direction of EWS) per bifurcation type and metric. Here, 100% of positive warning signs means that all warnings showed an increase, 0% means that all showed a decrease, and 50% means an equal mix of increases and decreases across f_s and σ_{obs} .

2.5 Implementation

All analyses were conducted using R Statistical Software (v4.2.1) [88]. Analysis code may be found in the package *bifurcationEWS* that accompanies the paper, freely accessible on GitHub [89], along with the full analysis scripts suitable for running on a High Performance Cluster.

Whereas the implementation of most selected EWS is rather straight-forward, the spectral EWS require some additional notes.

The maximum spectral density S_{\max} is computed by translating the Python code from the package *ewstools* [90] to R. The power spectrum was computed using Welch’s method with long-mean detrending as implemented in the function *pwelch* from the package *gsignal* [91].

Following [3], the spectral ratio is computed from a parametric estimate of the power spectrum using the *spec.ar* function from the package *stats* [88]. The order of the fitted autoregressive model is determined by the Akaike information criterion and thus determined per time series. As recommended by [3], the high frequency was set to the maximum possible for a given downsampling frequency f_s . The low frequency could not be set to 2.5 observations as recommended in case of $f_s = .1$, such that it instead was set to 10% of the high frequency. This yields the spectral ratio between a low frequency $\frac{f_s}{2 \cdot 10}$ and high frequency $\frac{f_s}{2}$.

Lastly, the spectral exponent is computed by translating the Matlab code from [76] to R. Though the recommended frequency band is $10^{-2} \geq f \leq 10^{-1}$ [92], this was not feasible given the lowest of our downsampling conditions $f_s = .1$. One alternative would be to estimate the slope on a fixed *percentage* of the frequency band. However, this has been shown to result in artefacts in the estimation of the slope [93]. A better method resulting in reliable slope estimates is to compute the slope on a fixed *amount* of lowest frequencies [93]. As such, we follow [76]’s computation of the spectral density, but compute the slope over the 50 lowest frequencies as recommended by [93].

3 Results

3.1 Bifurcation diagrams

Fig. 2 displays the bifurcation diagram of X_1 for the complete range of $s \in [.6, 1.3]$. As indicated by the

coloured background, the regimes traversed by the system vary greatly across the parameter space. Furthermore, it highlights the consistency of regime boundaries across all variables. Apparently, these connectivity strengths are strong enough for the critical bifurcation points to converge across variables, whereas for weakly connected systems, variables may bifurcate at different points in the parameter space [73].

Comparing the bifurcation diagrams per variable (Supplementary Figure S2) further demonstrates the variation in how the same regime is realised: differences in magnitude, timing, and periodicity make the GLV a truly challenging multidimensional system. For instance, the maximum value attained by x_3 is much lower than the other variables, and also displays a much simpler dampening oscillation before it reaches the fixed point it eventually settles in ($s \approx 1.22$). From this diagram alone, it is thus already to be expected that the univariate EWS do not show the same patterns across x_i . The bifurcation diagrams of the other three variables (Supplementary Figure S2), of $s \in [1.3, .6]$ (reverse order of s , Supplementary Figure S3), and of the saddle-node bifurcation (Supplementary Figure S4) may be found in the Supplementary Materials.

3.2 Predictability of bifurcations

The median AUC across conditions (downsampling frequency $f_s \in [10, 1, .1]$ and observational noise intensity $\sigma_{\text{obs}} \in [0.0001, .02, .04]$) is shown in Fig. 3. Strikingly, many EWS show near-perfect performance ($.9 \leq \text{AUC} \leq 1$, bright yellow) for about a third of bifurcations. Bifurcations which are more difficult to anticipate are of higher periodicity, such as period-doubling 4–8 and 8–16 and period-halving 16 to 8 and 8 to 4 (see Sect. 4.2.3 for an explanation of $\text{AUC} < .5$). Similarly, chaotic bifurcations, such as the period-doubling and period-halving cascade are hard to anticipate, involving transitions to or from attractors of high periodicity. Conversely, other chaotic bifurcations are remarkably easy to anticipate, such as the boundary and interior crisis (chaos expansion and chaos reduction), and subductions to a lesser extent.

The dependence of the AUC on downsampling frequency f_s and observational noise intensity σ_{obs} is shown in the Supplementary Materials. For simple transitions from fixed-points such as the saddle-node bifurcation, lower sampling frequency and greater observa-

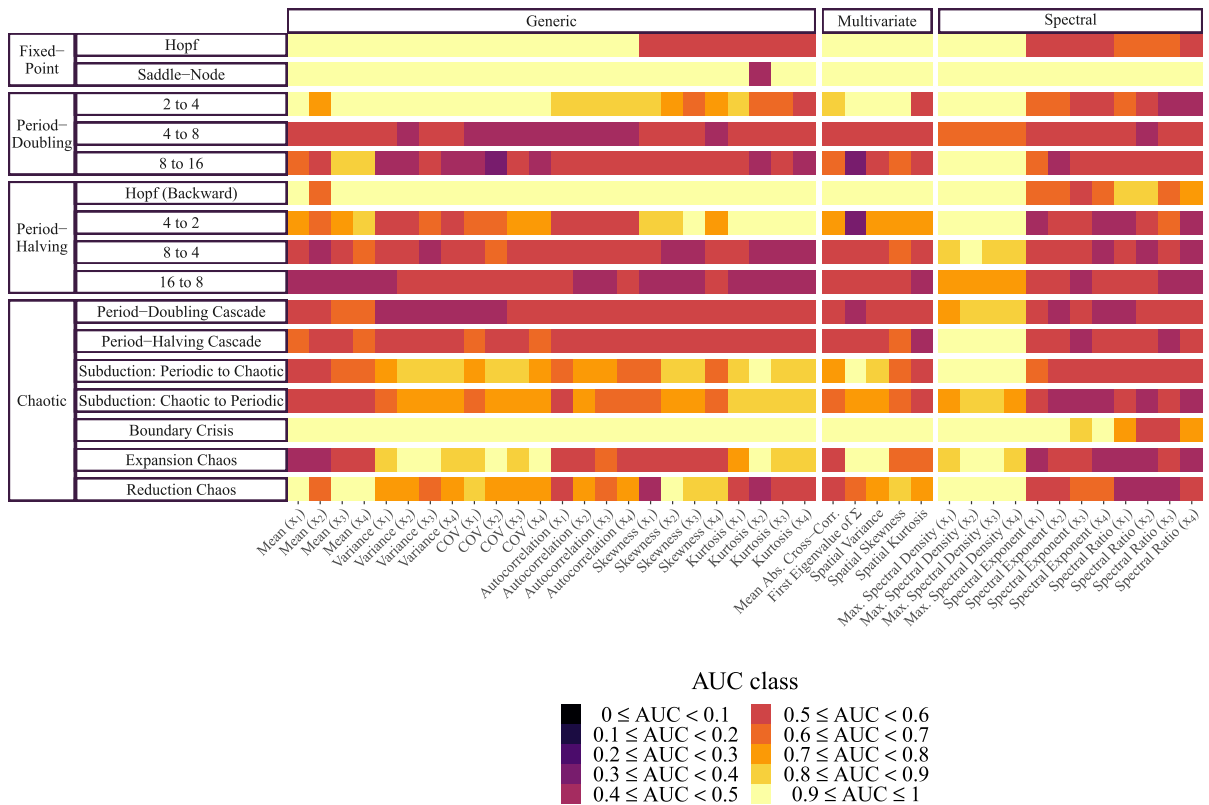


Fig. 3 Bifurcation-dependent performance of EWS. EWS performance is here visualised aggregated across conditions using the median AUC; for the AUC per condition (downsampling frequency $f_s \in [10, 1, .1]$ and observational noise intensity $\sigma_{\text{obs}} \in [0.0001, .02, .04]$), see Supplementary Figures S6–S11. Bifurcations involving fixed points (e.g. Hopf) seem remarkably easy to anticipate (bright yellow), whereas period-doubling and

period-halving are much harder to anticipate (red and purple). The EWS maximum spectral density S_{max} performs exceptionally well (bright yellow, light orange) for all bifurcation types. Note that $\text{AUC} < .5$ is due to the detection method not being suitable to identify complex warning patterns such as a reduction in variance, see Sect. 4.2.3. (Color figure online)

tional noise intensity barely changes the performance of EWS. In contrast, bifurcations of high periodicity are easily obscured by noise, even with high sampling frequency. Period-doubling and period-halving bifurcations are theoretically predictable as half of the EWS perform well under low observational noise intensity $\sigma_{\text{obs}} = 0.0001$, even for very low sampling frequencies $f_s = .1$ (except the period-halving bifurcation 16 to 8, which shows poor predictability across all conditions). However, higher observational noise intensities easily obscure these transitions, as a period-doubling or period-halving bifurcation often involves the gradual splitting or merging of peaks in the oscillation.

A different dependence on f_s and σ_{obs} emerges for chaotic bifurcations. EWS for the period-doubling and period-halving cascade to chaos show poor perfor-

mance across all conditions. In contrast, EWS for subductions (chaotic to periodic and periodic to chaotic) show remarkably good performance across conditions, where performance is only completely hindered in the most difficult condition $f_s = .1, \sigma_{\text{obs}} = .04$.

The most striking EWS across bifurcations is the maximum spectral density S_{max} , showing near-perfect performance ($.9 \leq \text{AUC} \leq 1$, bright yellow) across virtually all bifurcations. Such generality is not found across the other EWS. Among multivariate EWS, the first eigenvalue of the covariance matrix Σ and spatial variance seem to perform well. Among univariate generic EWS, no consistent best-performing EWS or signature is found, in line with the literature [94,95]. Though each metric shows somewhat consistent results among variables, outliers are also com-

mon. For instance, the mean of x_2 shows poor performance for detecting an interior crisis (chaos reduction), whereas this same metric applied to the other variables performs excellently. In line with this, several simulation studies have observed the (moderate) superiority of multivariate over univariate EWS [43, 84, 96].

3.3 Timing and direction of EWS

For practical utility, EWS should not only have high sensitivity and specificity, but also be *timely*. An EWS may have a perfect AUC ≈ 1 , but only yield a warning signal shortly before the transition, greatly reducing its utility. As a next step, we thus investigate whether an optimised critical cut-off value (for each bifurcation type, EWS, downsampling frequency f_s and σ_{obs}) which weighs sensitivity and specificity equally results in timely warning signals. As shown in Fig. 4, the majority of EWS occurred in the middle of the transitional period. Nearly half of the EWS for the saddle-node bifurcation only gave a very late warning. The maximum spectral density S_{max} again shows up as a strong warning—and timely—signal.

In the application of EWS, not only the timing but the *direction* of EWS matters. Do we need to look for a warning signal which peaks above the confidence band (i.e. an increase), below (i.e. a decrease), or either one? To investigate the sign of the warning signal, we found the direction of each warning sign corresponding to an optimised critical cut-off value per bifurcation type, EWS, downsampling frequency f_s and σ_{obs} . Remarkably, many EWS do not show warning signs that are either all increasing or all decreasing, but rather a mix (Supplementary Figure S12). For instance, a period-doubling cascade to chaos does not have a typical warning signature in which Spatial Variance either increases or decreases. Instead, either may be taken as a warning sign. As an implication, only looking for an increase or a decrease as compared to baseline might lead to more false negatives.

4 Discussion

In summary, anticipating complex critical transitions shows variable promise, depending on the type of critical transition and the EWS used. Generic EWS can pick up on an upcoming transition even in the absence

of critical slowing down. By studying the ideal case of a well-behaved bifurcation with ample data available, we learn which critical transitions are in principle foreseeable. Our findings may be broadly summarised as follows:

1. Bifurcations involving fixed points are extremely easy to anticipate, despite low sampling frequency or strong observational noise.
2. Bifurcations involving limit cycles of higher periodicity (4–8 and 8–16) are hard to predict and easily obscured by observational noise.
3. Chaotic bifurcations involving crises and subductions are much easier to detect than chaotic period-doubling and period-halving cascades.
4. The maximum spectral density S_{max} performs exceptionally well across virtually all bifurcation types, whereas other spectral EWS do not perform well at all.
5. Most well-performing EWS give a timely warning halfway into the transition, but many EWS do not have a consistent direction (increasing or decreasing as compared to the baseline).

4.1 Reasons for EWS in deterministic dynamics

The classical conception of warning signs for bifurcations focuses on measuring a loss of stability which is reflected in CSD. This loss of stability may be indirectly measured through the system's response to noise: closer to a bifurcation point, the system is less quick to recover from perturbations, resulting in the well-known rise in variance and autocorrelation. As such, some intrinsic noise is needed to uncover this loss of stability. Yet in the present study, even deterministic dynamics show warning signs of upcoming bifurcations, which are strong enough to be picked up even through observational noise and downsampling. Below, we delve into three perspectives on why some complex critical transitions in a deterministic system show EWS despite the absence of perturbations (see summary Fig. 5): changing attractor morphology (size, shape, and location in phase landscape), shifting power spectra (amplitude and frequency), and chaotic transitional features (density across attractor). These features are not commonly connected to EWS given the focus on CSD, but are in fact simple characteristics of deterministic dynamics. They may occur independently, in combination, or not at all across complex transitions. Importantly, when we

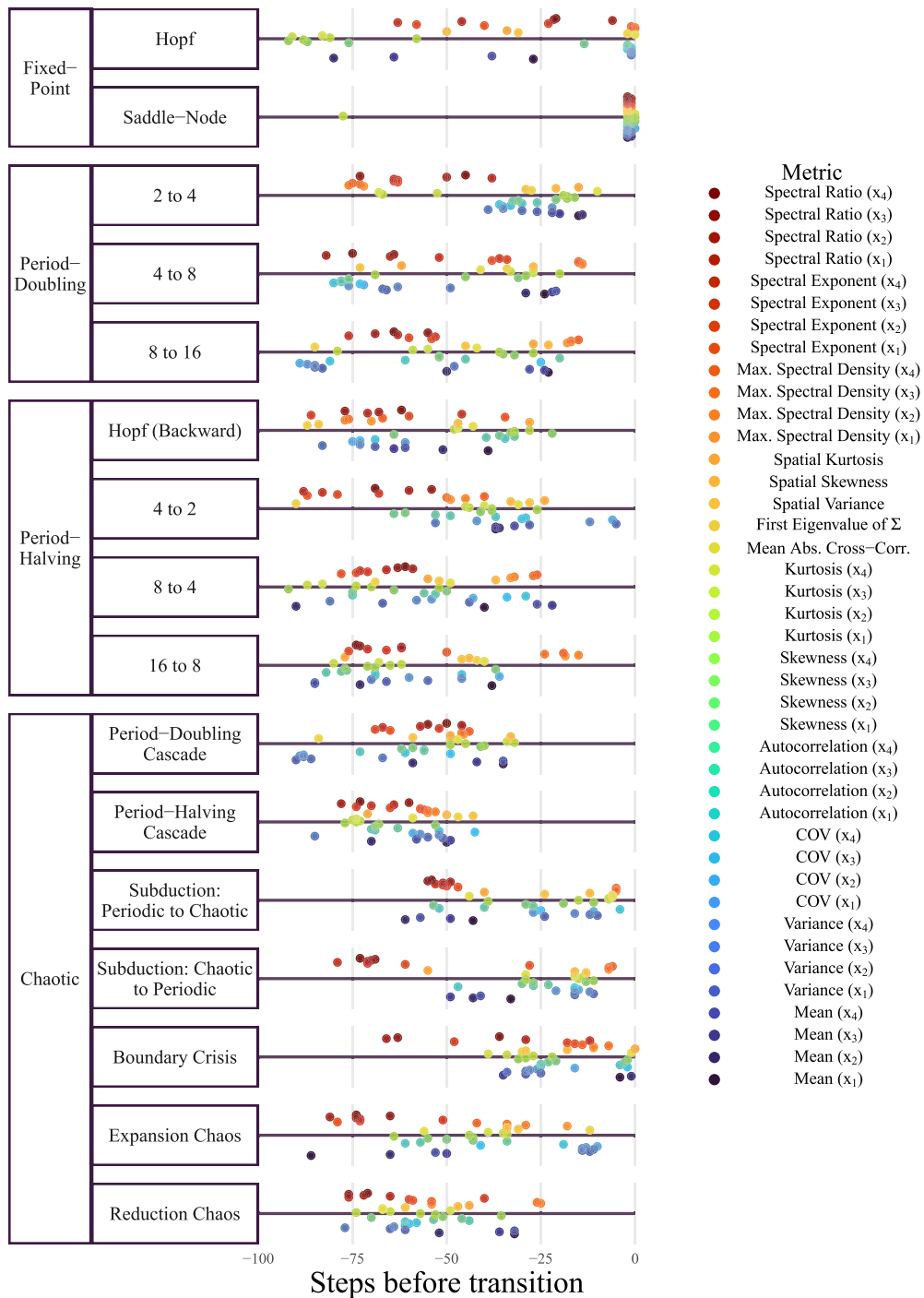


Fig. 4 Timing of EWS when setting an optimal cut-off value σ_{crit}^* with optimal sensitivity and specificity for each EWS. Timing of EWS is here visualised aggregated across conditions (down-sampling frequency f_s and observational noise intensity σ_{obs}) using the median timing. Across different bifurcation types, the

majority of EWS yield timely warnings: about 25–75 steps in the control parameter before the transition occurs. An exception is the saddle-node bifurcation, which is announced very late by virtually all EWS. Note that the points are vertically jittered to improve visibility

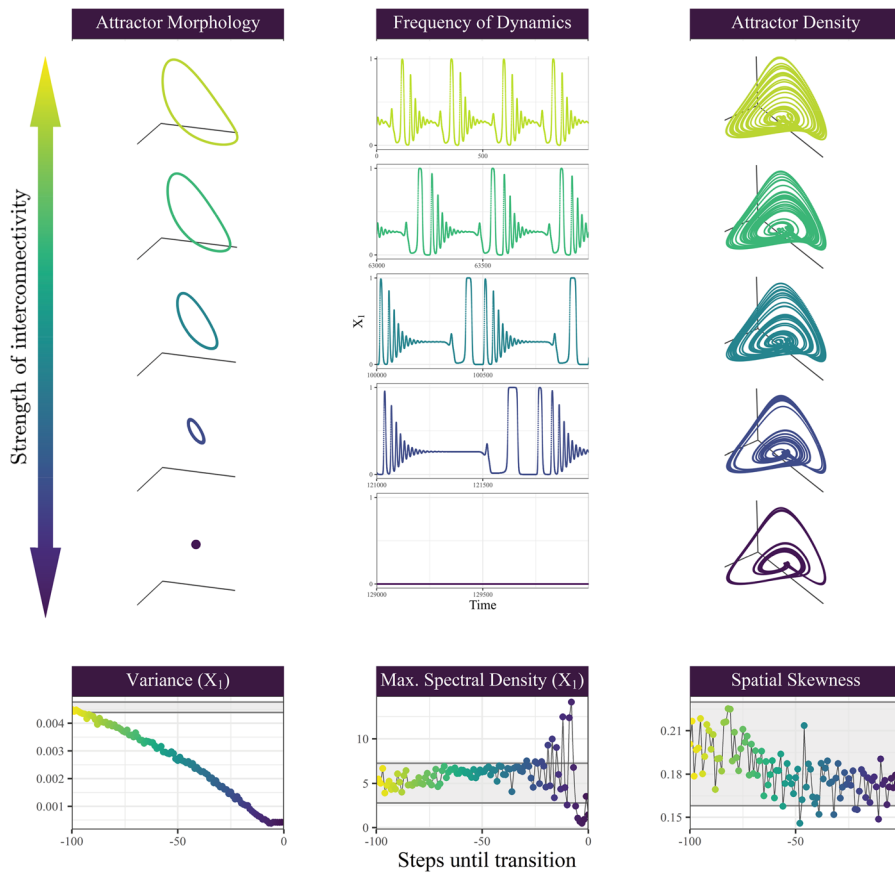


Fig. 5 Reasons for EWS in deterministic dynamics. (1) Changing attractor morphology refers to the gradual alterations in the size, shape, and location of the attractor in phase space, as demonstrated by the backwards Hopf bifurcation (left, top panel). Such changes are easily picked up by EWS such as variance x_1 (left, bottom panel). (2) Changes in the frequency of dynamics can result in power spectral changes, here visualised for the boundary crisis (middle, top panel), which are easily picked up by power spectral EWS such as the maximum spectral density S_{\max}

of x_1 (middle, bottom panel). (3) Chaotic bifurcations such as an interior crisis (larger chaotic attractor to smaller chaotic attractor) (right, top panel) may be accompanied by transitional features such as differing density across the attractor. EWS such as spatial skewness can reflect this transitional process (right, bottom panel). All EWS shown are for downsampling frequency $f_s = 1$ and observational noise intensity $\sigma_{\text{obs}} = .02$, with confidence bands constructed from a baseline period (not shown) with $\sigma_{\text{crit}} = 2$

do not know which type of transition will occur, implementing a range of EWS may be necessary as different metrics may be sensitive to different features of complex transitions.

4.1.1 Phase space perspective: changing attractor morphology

Besides the loss of stability, an upcoming bifurcation is often accompanied by changes in the morphology of the attractor: its location, size, and shape in state space. These morphological properties are reflected in statisti-

cal metrics of the time series, most straight-forwardly in the mean, variance, and skewness, respectively. Importantly, the morphology of an attractor can be used as a warning sign of an upcoming bifurcation, because it often changes gradually and smoothly along with the changing control parameter. For instance, a limit cycle approaching a supercritical Hopf bifurcations in the reverse direction slowly shrinks in amplitude, which can easily be picked up by steadily decreasing variance (Fig. 5, left panel). Similarly, period-doubling transitions are often preceded by a gradually growing attractor (Fig. 5, left panel). This phenomenon has also been

called critical attractor growth as a warning sign of an upcoming interior crisis [59].

Concomitant changes in the attractor's morphology as the system approaches a bifurcation have perhaps received little attention in the literature given its focus on fixed points, for which only the location in state space (i.e. mean) may change. A gradually changing mean may be observed in a saddle-node bifurcation or backwards supercritical and transcritical bifurcations. Our ability to pick up these changes will of course depend on the level of noise and the magnitude and rate of change of the control parameter—mean changes may be too small to detect, and some bifurcations may happen without any change at all in the attractor's morphology. However, for most bifurcations under study, and particularly for intrinsically dynamic attractors, gradually changing attractor morphology may be a fruitful warning sign of an upcoming bifurcation.

4.1.2 Power spectrum perspective: changing amplitude and frequency

Emerging as by far the most effective and universal EWS, the maximum spectral density S_{\max} [9] illustrates that spectral warning signals may already be present in deterministic dynamics. This cannot be explained by only an increase in variance, as variance as an EWS did not perform nearly as well (Fig. 3). As explained by [9], in cases where the bifurcation involves an oscillatory attractor, non-spectral EWS may not be useful. Indeed, a warning sign may not (only) be in the shape of an attractor, but in the *speed at which it traverses* the attractor. Non-linear systems typically have attractors with phase-dependent velocity, meaning some parts of the oscillation are quicker than others (Fig. 5, middle panel) [97]. Some bifurcations, such as the backwards Hopf bifurcation, are announced by an increased uniformity in the speed along the attractor, becoming less phase-dependent [97, 98]. Phase-dependent velocity may change along with a control parameter, particularly when the control parameter affects growth rates or connectivity of the system [47, 48, 99]. Increasing interspecies competition can result in more extreme peaks and troughs and slower recovery, as seen in the boundary crisis (Fig. 5, middle panel). Changes in the speed with which the system traverses an attractor may be picked up by the power spectrum, which describes the distribution of variance across different frequencies. For instance, gradually increasing amplitudes

are reflected by overall increased spectral power (i.e. amplitude squared), and a slowing down of dynamics will be shown by a shift of spectral power towards lower frequencies. As such, our findings corroborate other recent findings on the utility of spectral EWS for bifurcations involving oscillatory dynamics [9, 36, 100].

Spectral EWS are thus an obvious candidate for anticipating bifurcations involving oscillatory attractors. In the EWS literature, they have predominantly been used for fixed point bifurcations in the context of *spectral reddening* [101], in which the power spectrum becomes dominated by lower frequencies near a bifurcation point. This is another manifestation of CSD, because lower frequencies imply slower recovery. The spectral ratio and spectral exponent were specifically designed to pick up on CSD and spectral reddening (higher spectral power at lower frequencies [101]), but performed quite poorly in the present study. This difference might simply be due to the method of estimating the power spectrum, ranging from Welch's method (maximum spectral density [9]), parametrically by an AR model (spectral ratio [3]), or the Fast Fourier Transform (spectral exponent [76, 102]). Another explanation for their poor performance may come from the chosen frequency bands, which could be optimized to detect relevant frequency changes in complex bifurcations. Some of the generic EWS also measure spectral reddening indirectly if they are intrinsically related to the power spectrum, where for instance the variance is simply the sum of the spectral power and the lag-1 autocorrelation forms a Fourier pair with the power spectrum [103].

4.1.3 Chaotic perspective: density across attractor

A third cause for EWS in deterministic dynamics may be observed in critical transitions involving chaotic attractors (Fig. 5, right panel). A bifurcation involving a chaotic attractor may be preceded by the system lingering longer and more frequently in some regions of the attractor. As any chaotic attractor forms the closure of a set of an infinite number of unstable periodic orbits, preference for some attractor regions manifests in density differences across the attractor. That is, the new attractor is already embedded within the current attractor, and typically the system lingers more and longer in the new attractor nearing a bifurcation. Attractor density differences may be driven by phenomena such as *intermittency*: recurrent switches between attractors

such as a periodic and a chaotic one (subduction) or two chaotic attractors (interior crisis; see Supplementary Materials section S1.1.3 and Supplementary Figure S1 for further explanation). Warning signs may be found in the duration and time between successive periodic bursts or increased density of a smaller attractor within a larger attractor, as they carry information about the system's proximity to a bifurcation point. That is, the new attractor typically gains prominence closer to the bifurcation point, such that the system frequents it more often and for longer periods of time, until it switches to the new attractor completely.

On a sobering note, these features depend strongly on the initial condition, rate of parameter change, and intrinsic noise [104], such that they are no guarantee for a warning signal. Similarly, other typical features of chaotic transitions occur quite robustly but are hard to detect. For instance, increased complexity is found reliably in the period-doubling route to chaos, yet may be of little utility. Here, we find that EWS barely distinguish between high periodicity and chaoticity if the system is already far into the period-doubling cascade.

4.2 Methodological implications

Below, we outline three methodological implications for EWS simulation studies that may be implied by our findings.

4.2.1 EWS are also contained within deterministic dynamics

The multitude of warning signals found in only deterministic dynamics emphasises the need for a step-wise understanding of complex bifurcations, which begins with deterministic dynamics and builds towards stochastic systems. Simulation studies in the EWS literature have predominantly focused on CSD: the slower recovery from state perturbations. To uncover this effect, a stochastic system is needed, which inescapably builds in assumptions about the noise process. Rather than being restricted to homogeneous additive Gaussian noise, the noise process may be coloured (red, pink, blue), multiplicative, time-varying, and anisotropic across variables. Indeed, deviations from these assumptions have often been found to negatively impact the utility of EWS, including correlated [105], anisotropic

[95], cyclical [106], and multiplicative state perturbations [107]. Deviations from these assumptions may help to explain the gap between theoretical expectations of EWS and empirical findings, which have found mixed results, receiving support [108–117], but also scepticism due to low true positive and/or high false positive rates, poor agreement between EWS, and cherry-picked variables and data sets [84, 94, 106, 118–124]. This gap may also originate from basic practical considerations, such as short time series length [125], pre-processing sensitivity [84], or insufficient spatial and temporal sampling [123], but also on more fundamental differences between simulated and empirical transitions. Empirical systems may not be as well-behaved as typical simulation models, including low noise [126], a single driver variable [127], or a slow timescale of the driver relative to intrinsic system dynamics [128, 129], or may be transitioning due to a different mechanism altogether, such as noise [122, 130], or large jumps in external forcing [63].

The interaction between deterministic dynamics and stochasticity may enhance or blunt EWS [107]. For instance, critical slowing down would only enhance the increased variance that is already present deterministically in some period-doubling bifurcations. Conversely, state perturbations help reveal warning signals in the form of stochastic resonance when approaching a Hopf bifurcation, which are not present in deterministic dynamics [9]. State perturbations can even limit what dynamics are *possible*. For instance, the period-doubling cascade to chaos is easily shortened [66] or even avoided altogether by state perturbations [131]. Stochasticity may thus reveal or hide the underlying deterministic skeleton. Though noise is always present in any empirical system, by first simulating a fully deterministic system and then adding stochasticity, we may disentangle which EWS are dependent on the assumed noise process.

4.2.2 EWS are not generic across bifurcations

In the early stages, optimism surrounding the utility of EWS was fuelled by their potential *generic* nature, meaning they are applicable to many types of transitions, without requiring knowledge of the underlying system [6, 53, 70]. The literature has increasingly adopted a more sceptical stance [47, 132]. The performance and pattern of EWS depends on the bifurcation type, system dimensionality, and control param-

ter characteristics, among many other factors. Firstly, the pattern of EWS can differ even within the same *family* of bifurcations. For example, though both the saddle-node and Hopf bifurcation are zero-eigenvalue bifurcations, a different pattern of EWS is expected when approaching the bifurcation point: for a saddle-node bifurcation, increasing lag-1 autocorrelation is observed, where it is shown to *decrease* approaching a Hopf bifurcation [9,35]. Secondly, even within the same bifurcation *type*, EWS findings in one system may not translate to another due to different system dimensionality and structure. In multidimensional systems, not all variables show the same strength of EWS [95], or may even show the completely opposite pattern [94]. And indeed, our intuitions about chaotic dynamics in one-dimensional models may not extend to higher dimensions [10], which are often the empirical reality when studying complex systems. For larger systems, depending on the coupling strength between different nodes in the network, perturbations to one node may not propagate to all nodes [133]. As such, weakly coupled systems may only show localised changes in behaviour. Theoretical work has supported the variability in EWS within the same system from a state space perspective, as the strength of EWS is influenced by at least four directions: the direction of critical slowing down, the direction of intrinsic noise, the direction along which noise has the strongest effect, and the direction along which the process is observed [95]. Thirdly, EWS patterns differ depending on the characteristics of the control parameter or driver. Though most studies assume a single, monotonically increasing driver, which in itself seems questionable [84], EWS signatures differ in the case of large jumps in the control parameter [63,84], multiple driver variables [127], and periodic forcing [106]. Empirically, drivers are likely a mixture of linear and non-linear variables [84,134,135].

Strengthening the established non-generic nature of EWS, our findings show no consistent performance across bifurcations nor a similar direction in the pattern of EWS (increasing or decreasing, Supplementary Figure S12) upon approaching a bifurcation. Moreover, our findings corroborate the danger in relying on warning signs derived from one state variable, as it may simply be the least informative variable in anticipating that particular critical transition. Combined with the overall literature, this implies that any EWS application should not rely a priori on only a few EWS, one direction (increasing or decreasing), or single state

variables. Further, simulation studies need a strong empirical basis underlying their modelling assumptions (e.g. bifurcation type, system dimensionality, and driver characteristics) before drawing general conclusions about the utility of EWS.

4.2.3 Complex warning signals need different detection methods

The present study demonstrates why conventional warning detection methods are not suitable for some complex bifurcations. Conventional methods detect a trend upwards or downwards, but complex bifurcations may show warnings in *higher-order* statistics of EWS. That is, rather than increasing or decreasing steadily, some EWS warn against a transition through a change in variance or frequency. For instance, attractors that oscillate also yield warning signals that oscillate (Supplementary Figure S13, top panel). Another complex warning pattern not picked up by conventional methods is a reduction in variance of EWS, which is common in period-halving bifurcations (Supplementary Figure S13, middle panel). In this case, the EWS will show *no* increases nor decreases, but rather a narrowing in variance, yielding no typical warning signal as identified by standard methods. Similarly, a change in the *frequency* of the EWS signal without a trend upwards or downwards is not recognized as a warning (Supplementary Figure S13, bottom panel), though such EWS signals are common in for instance period-doubling bifurcations. Such complex patterns lead to the atypical result of $AUC < .5$: as the critical cut-off value increases, the number of true positives drops *before* the number of false positives.

Complex warning patterns thus pose a challenge to current detection methods, without straight-forward methodological solutions. For instance, one proposal to increase the robustness of EWS suggests to only count a warning if there are multiple *consecutive* warnings signals [136]. For an oscillating EWS which intrinsically will first peak above and then dip below the threshold (Supplementary Figure S13, top panel), this might lead to sluggish detection. The same problem would arise when using another popular warning detection method, Kendall's τ [77,137], which identifies an increasing or decreasing trend. Potential techniques to deal with these complex warning patterns might come from statistical process control [138,139], utilizing smoothing as well as secondary statistics, e.g. the

variance of the variance x_1 . However, rather than relying on single EWS, a much more promising approach comes from machine-learning techniques, which have demonstrated excellent utility in anticipating bifurcations [15, 140, 141]. Machine-learning algorithms such as deep learning may be trained on raw time series and extract relevant (higher-order) features for predicting a bifurcation, without relying on manual specification of relevant EWS.

5 Conclusion

The present study aimed to highlight warning signals contained within deterministic dynamics to build a step-wise understanding of the largely understudied domain of complex bifurcations. The focus on fixed-point bifurcation has left little attention for warning signs that may already be found in deterministic dynamics of complex attractors such as limit cycles and chaotic attractors. Such warning signs may be found in a combination of changing attractor morphology (size, shape, and location in phase space), power spectra (amplitude and frequency), and chaotic transitional characteristics (density across attractor). A step-wise understanding starts from the simplest case: What fluctuations in EWS can we expect simply from deterministic dynamics in null models? How will these deterministic dynamics change when approaching a bifurcation? After understanding the deterministic transitional process, we may better understand the stochastic bifurcation: how are these warnings obscured—or conversely, amplified—when subject to dynamical noise? The present study suggests that future studies investigating these questions may be more informative by comparing deterministic to stochastic dynamics, by adjusting the warning detection method to account for oscillations, and by aiming for a comprehensive simulation design to avoid system-specific and bifurcation-specific conclusions.

Our findings highlight the divergent predictability found among bifurcations, where for instance transitions involving attractors of high periodicity are much harder to anticipate than simpler bifurcations. This should warrant scepticism towards general statements about the utility of EWS, and in particular the pes-

simism with regard to chaotic bifurcations. There is no such thing as *one* type of chaotic critical transition. Rather, a rich array of underlying phase space structures may cause a bifurcation. This diversity calls for an overview on the utility of EWS depending on structural factors (e.g. type of system, type of critical transition), methodological factors (e.g. pre-processing protocol and type of EWS), and practical factors (e.g. length and frequency of measurement). The choice of categorization among structural factors alone already poses a challenge, where the need to aggregate across similar features (e.g. period-doubling bifurcations) conflicts with the need to distinguish between relevant features (e.g. different origins of chaos). In addition, the choice of what qualifies as a transition and what is considered a warning signal is somewhat subjective. For instance, are period-doubling bifurcations transitions of interest in themselves, or do they merely serve as warning signs of oncoming chaos [66]? Vice versa, intermittency in some systems would not be considered as part of the transition process to the true attractor of interest, but rather a switch in itself with severe consequences. Depending on the aim, some critical transitions may thus be considered transitional features and vice versa.

Author contributions Conceptualization: Kyra Evers, Lourens Waldorp, Denny Borsboom, Eiko Fried, Fred Hasselman; Methodology: Kyra Evers, Lourens Waldorp, Denny Borsboom, Eiko Fried, Fred Hasselman; Software: Kyra Evers; Formal analysis: Kyra Evers; Writing—Original Draft: Kyra Evers; Writing—Review and Editing: Kyra Evers, Lourens Waldorp, Denny Borsboom, Eiko Fried, Fred Hasselman; Visualization: Kyra Evers; Supervision: Lourens Waldorp, Denny Borsboom, Eiko Fried, Fred Hasselman; Funding acquisition: Lourens Waldorp, Denny Borsboom

Funding This study is part of the project ‘New Science of Mental Disorders’ (www.nsmdeu), supported by the Dutch Research Council and the Dutch Ministry of Education, Culture and Science (NWO gravitation Grant Number 024.004.016). Denny Borsboom is supported by Dutch Research Council Grant V.I.C.181.029.

Availability of data and materials Example data sets are available in the package *bifurcationEWS* that accompanies the paper, freely accessible on GitHub at <https://github.com/KCEvers/bifurcationEWS>.

Code availability R code can be found in the package *bifurcationEWS* that accompanies the paper, freely accessible on GitHub at <https://github.com/KCEvers/bifurcationEWS>.

Declarations

Conflict of interest The authors have no relevant financial or non-financial interests to disclose. The authors declare no Conflict of interest.

Ethics approval Not applicable.

Consent to participate Not applicable.

Consent for publication Not applicable.

Open Access This article is licensed under a Creative Commons Attribution 4.0 International License, which permits use, sharing, adaptation, distribution and reproduction in any medium or format, as long as you give appropriate credit to the original author(s) and the source, provide a link to the Creative Commons licence, and indicate if changes were made. The images or other third party material in this article are included in the article's Creative Commons licence, unless indicated otherwise in a credit line to the material. If material is not included in the article's Creative Commons licence and your intended use is not permitted by statutory regulation or exceeds the permitted use, you will need to obtain permission directly from the copyright holder. To view a copy of this licence, visit <http://creativecommons.org/licenses/by/4.0/>.

References

- Scheffer, M., Carpenter, S.R., Lenton, T.M., Bascompte, J., Brock, W., Dakos, V., Koppel, J.V.D., Leemput, I.A.V.D., Levin, S.A., Nes, E.H.V., Pascual, M., Vandermeer, J.: Anticipating critical transitions. *Science* **338**, 344–348 (2012). <https://doi.org/10.1126/science.1225244>
- Hastings, A., Abbott, K.C., Cuddington, K., Francis, T., Gellner, G., Lai, Y.C., Morozov, A., Petrovskii, S., Scranton, K., Zeeman, M.L.: Transient phenomena in ecology. *Science* (2018). <https://doi.org/10.1126/science.aat6412>
- Biggs, R., Carpenter, S.R., Brock, W.A.: Turning back from the brink: detecting an impending regime shift in time to avert it. *Proc. Natl. Acad. Sci.* **106**, 826–831 (2009). <https://doi.org/10.1073/pnas.0811729106>
- Gilmore, R.: *Catastrophe Theory*. Wiley, London (2007). <https://doi.org/10.1002/3527600434.eap052.pub2>
- Wissel, C.: A universal law of the characteristic return time near thresholds. *Oecologia* **65**, 191–197 (1984). <https://doi.org/10.1007/BF00384470>
- Scheffer, M., Bascompte, J., Brock, W.A., Brovkin, V., Carpenter, S.R., Dakos, V., Held, H., Nes, E.H.V., Rietkerk, M., Sugihara, G.: Early-warning signals for critical transitions. *Nature* **461**, 53–59 (2009). <https://doi.org/10.1038/nature08227>
- Kelso, J.A.S.: Instabilities and phase transitions in human brain and behavior. *Front. Hum. Neurosci.* (2010). <https://doi.org/10.3389/fnhum.2010.00023>
- Haken, H.: *Synergetics: An Introduction: Nonequilibrium Phase Transitions and Self-Organization in Physics, Chemistry, and Biology*. Springer, Berlin (1978)
- Bury, T.M., Bauch, C.T., Anand, M.: Detecting and distinguishing tipping points using spectral early warning signals. *J. R. Soc. Interface* (2020). <https://doi.org/10.1098/rsif.2020.0482>
- Munch, S.B., Brias, A., Sugihara, G., Rogers, T.L.: Frequently asked questions about nonlinear dynamics and empirical dynamic modelling. *ICES J. Mar. Sci.* **77**, 1463–1479 (2020). <https://doi.org/10.1093/icesjms/fsz209>
- Nes, E.H.V., Scheffer, M.: Large species shifts triggered by small forces. *Am. Nat.* **164**, 255–266 (2004). <https://doi.org/10.1086/422204>
- Voorn, G.A.K.V., Kooi, B.W., Boer, M.P.: Ecological consequences of global bifurcations in some food chain models. *Math. Biosci.* **226**, 120–133 (2010). <https://doi.org/10.1016/J.MBS.2010.04.005>
- Dakos, V., Soler-Toscano, F.: Measuring complexity to infer changes in the dynamics of ecological systems under stress. *Ecol. Complex.* **32**, 144–155 (2017). <https://doi.org/10.1016/j.ecocom.2016.08.005>
- Rikkert, M.G.M.O., Dakos, V., Buchman, T.G., Boer, R.D., Glass, L., Cramer, A.O.J., Levin, S., Nes, E.V., Sugihara, G., Ferrari, M.D., Tolner, E.A., Leemput, I.V.D., Lagro, J., Melis, R., Scheffer, M.: Slowing down of recovery as generic risk marker for acute severity transitions in chronic diseases. *Crit. Care Med.* **44**, 601–606 (2016). <https://doi.org/10.1097/CCM.0000000000001564>
- Deb, S., Bhandary, S., Sinha, S.K., Jolly, M.K., Dutta, P.S.: Identifying critical transitions in complex diseases. *J. Biosci.* (2022). <https://doi.org/10.1007/S12038-022-00258-7>
- Trefois, C., Antony, P.M.A., Goncalves, J., Skupin, A., Balling, R.: Critical transitions in chronic disease: transferring concepts from ecology to systems medicine. *Curr. Opin. Biotechnol.* **34**, 48–55 (2015). <https://doi.org/10.1016/J.COPBIO.2014.11.020>
- Uthamacumaran, A.: A review of dynamical systems approaches for the detection of chaotic attractors in cancer networks. *Patterns* (2021). <https://doi.org/10.1016/j.patter.2021.100226>
- Nazarimehr, F., Mohammad, S., Golpayegani, R.H., Hatef, B.: Does the onset of epileptic seizure start from a bifurcation point? *Eur. Phys. J. Spec. Top.* **227**, 697–705 (2018). <https://doi.org/10.1140/epjst/e2018-800013-1>
- Schiepek, G.: Complexity and nonlinear dynamics in psychotherapy. *Eur. Rev.* **17**, 331–356 (2009). <https://doi.org/10.1017/S1062798709000763>
- Schiepek, G., Schöller, H., Felice, G., Steffensen, S.V., Bloch, M.S., Fartacek, C., Aichhorn, W., Viol, K.: Convergent validation of methods for the identification of psychotherapeutic phase transitions in time series of empirical and model systems. *Front. Psychol.* (2020). <https://doi.org/10.3389/fpsyg.2020.01970>
- Olthof, M., Hasselman, F., Maatman, F., Bosman, A., Lichtwarck-Aschoff, A.: Complexity theory of psychopathology. *J. Psychopathol. Clin. Sci.* **132**, 314–323 (2023). <https://doi.org/10.31234/osf.io/f68ej>
- Abel, A., Hayes, A.M., Henley, W., Kuyken, W.: Sudden gains in treatment resistant depression sudden gains in cognitive behavior therapy for treatment resistant depression: Processes of change. *J. Consult. Clin. Psychol.* **84**, 726–737 (2016). <https://doi.org/10.1037/ccp0000101>

23. Helmich, M.A., Olthof, M., Oldehinkel, A.J., Wichers, M., Bringmann, L.F., Smit, A.C.: Early warning signals and critical transitions in psychopathology: challenges and recommendations. *Curr. Opin. Psychol.* **41**, 51–58 (2021). <https://doi.org/10.1016/j.copsyc.2021.02.008>
24. Nishith, P., Resick, P.A., Griffin, M.G.: Pattern of change in prolonged exposure and cognitive-processing therapy for female rape victims with posttraumatic stress disorder. *J. Consult. Clin. Psychol.* **70**, 880–886 (2002). <https://doi.org/10.1037//0022-006x.70.4.880>
25. Hayes, A.M., Laurenceau, J.P., Feldman, G., Strauss, J.L., Cardaciotto, L.A.: Change is not always linear: the study of nonlinear and discontinuous patterns of change in psychotherapy. *Clin. Psychol. Rev.* **27**, 715 (2007). <https://doi.org/10.1016/J.CPR.2007.01.008>
26. Strunk, G., Lichtwarck-Aschoff, A.: Therapeutic chaos. *J. Person-Oriented Res.* **5**, 81–100 (2019). <https://doi.org/10.17505/jpor.2019.08>
27. Thompson, J.M.T., Sieber, J.: Predicting climate tipping as a noisy bifurcation: a review. *Int. J. Bifurc. Chaos* **21**, 399–423 (2011). <https://doi.org/10.1142/S0218127411028519>
28. Fontich, E., Guillamon, A., Lázaro, J.T., Alarcón, T., Vidiella, B., Sardanyés, J.: Critical slowing down close to a global bifurcation of a curve of quasi-neutral equilibria. *Commun. Nonlinear Sci. Numer. Simul.* (2022). <https://doi.org/10.1016/j.cnsns.2021.106032>
29. Lynch, S.: *Dynamical Systems with Applications Using MATLAB*, 2nd edn. Springer, Berlin (2014)
30. Dubitzky, W., Wolkenhauer, O., Cho, K.-H., Yokota, H. (eds.): *Encyclopedia of Systems Biology*. Springer, New York (2013). <https://doi.org/10.1007/978-1-4419-9863-7>
31. Hastings, A., Wysham, D.B.: Regime shifts in ecological systems can occur with no warning. *Ecol. Lett.* **13**, 464–472 (2010). <https://doi.org/10.1111/j.1461-0248.2010.01439.x>
32. Strogatz, S.: *Nonlinear Dynamics and Chaos: With Applications to Physics, Biology, Chemistry, and Engineering*. CRC Press, Boca Raton (1994)
33. Lorenz, E.N.: Deterministic nonperiodic flow. *J. Atmos. Sci.* **20**, 130–141 (1963)
34. Carpenter, S.R., Brock, W.A.: Early warnings of regime shifts in spatial dynamics using the discrete Fourier transform. *Ecosphere* (2010). <https://doi.org/10.1890/ES10-00016.1>
35. Dakos, V., Glaser, S.M., Hsieh, C.H., Sugihara, G.: Elevated nonlinearity as an indicator of shifts in the dynamics of populations under stress. *J. R. Soc. Interface* (2017). <https://doi.org/10.1098/RSIF.2016.0845>
36. Williamson, M.S., Lenton, T.M.: Detection of bifurcations in noisy coupled systems from multiple time series. *Chaos* (2015). <https://doi.org/10.1063/1.4908603>
37. Tirabassi, G., Masoller, C.: Correlation lags give early warning signals of approaching bifurcations. *Chaos Solitons Fractals* (2022). <https://doi.org/10.1016/j.chaos.2021.111720>
38. Adamson, M.W., Dawes, J.H.P., Hastings, A., Hilker, F.M.: Forecasting resilience profiles of the run-up to regime shifts in nearly-one-dimensional systems. *J. R. Soc. Interface* (2020). <https://doi.org/10.1098/rsif.2020.0566>
39. Vano, J.A., Wildenberg, J.C., Anderson, M.B., Noel, J.K., Sprott, J.C.: Chaos in low-dimensional Lotka–Volterra models of competition. *Nonlinearity* **19**, 2391–2404 (2006). <https://doi.org/10.1088/0951-7715/19/10/006>
40. Barabás, G., Michalska-Smith, M.J., Allesina, S.: The effect of intra- and interspecific competition on coexistence in multispecies communities. *Am. Nat.* **188**, 1–12 (2016). <https://doi.org/10.1086/686901>
41. Murray, J.D.: *Mathematical Biology*, 2nd edn. Springer, Berlin (1993). <https://doi.org/10.1007/978-3-662-08542-4>
42. May, R.M.: Biological populations with nonoverlapping generations: stable points, stable cycles, and chaos. *New Ser.* **186**, 645–647 (1974)
43. Dakos, V.: Identifying best-indicator species for abrupt transitions in multispecies communities. *Ecol. Indic.* (2018). <https://doi.org/10.1016/j.ecolind.2017.10.024>
44. Maas, H.L.J.V.D., Dolan, C.V., Grasman, R.P.P.P., Wicherts, J.M., Huizenga, H.M., Raijmakers, M.E.J.: A dynamical model of general intelligence: the positive manifold of intelligence by mutualism. *Psychol. Rev.* **113**, 842–861 (2006). <https://doi.org/10.1037/0033-295X.113.4.842>
45. Malcai, O., Biham, O., Richmond, P., Solomon, S.: Theoretical analysis and simulations of the generalized Lotka–Volterra model. *Phys. Rev. E* (2002). <https://doi.org/10.1103/PhysRevE.66.031102>
46. Sterpu, M., Rocşoreanu, C., Soava, G., Mehedintu, A.: A generalization of the grey Lotka–Colterra model and application to GDP, export, import and investment for the European Union. *Mathematics* (2023). <https://doi.org/10.3390/math11153351>
47. Dablander, F., Pichler, A., Cika, A., Bacilieri, A.: Anticipating critical transitions in psychological systems using early warning signals: theoretical and practical considerations. *Psychol. Methods* **28**, 765–790 (2022). <https://doi.org/10.1037/MET0000450>
48. Leemput, I.A.V.D., Wichers, M., Cramer, A.O.J., Borsboom, D., Tuerlinckx, F., Kuppens, P., Nes, E.H.V., Viechtbauer, W., Giltay, E.J., Aggen, S.H., Derom, C.: Critical slowing down as early warning for the onset and termination of depression. *PNAS* (2014). <https://doi.org/10.1073/pnas.1312114110>
49. Allesina, S., Tang, S.: The stability-complexity relationship at age 40: a random matrix perspective. *Popul. Ecol.* **57**, 63–75 (2015). <https://doi.org/10.1007/s10144-014-0471-0>
50. Voorn, G.A.K.: *Tipping Points in Natural Systems. An Inventory of Types, Early Warnings, and Consequences*. Wageningen University, Wageningen (2012)
51. Lai, Y.-C., Tél, T.: *Transient Chaos: Complex Dynamics on Finite Time Scales*, 1st edn. Springer, New York (2011). <https://doi.org/10.1007/978-1-4419-6987-3>
52. Ott, E.: *Chaos in Dynamical Systems*. Cambridge University Press, Cambridge (1983)
53. Kéfi, S., Dakos, V., Scheffer, M., Nes, E.H.V., Rietkerk, M., Kéfi, S., Scheffer, M., Nes, E.H.V.: Early warning signals also precede non-catastrophic transitions. *Oikos* **122**, 641–648 (2013). <https://doi.org/10.1111/j.1600-0706.2012.20838.x>
54. Batt, R.D., Brock, W.A., Carpenter, S.R., Cole, J.J., Pace, M.L., Seekell, D.A.: Asymmetric response of early warning indicators of phytoplankton transition to and from cycles. *Thyroid Res.* **6**, 285–293 (2013). <https://doi.org/10.1007/s12080-013-0190-8>

55. Gopalakrishnan, E.A., Sharma, Y., John, T., Dutta, P.S., Sujith, R.I.: Early warning signals for critical transitions in a thermoacoustic system. *Sci. Rep.* (2016). <https://doi.org/10.1038/srep35310>
56. Hao, B.-L.: Universal slowing down exponent near period-doubling bifurcation points. *Phys. Lett.* (1981). <https://doi.org/10.1007/s10955-005-8669-3>
57. Hao, B.: Critical slowing down in one-dimensional maps and beyond. *J. Stat. Phys.* **121**, 749–757 (2005). <https://doi.org/10.1007/s10955-005-8669-3>
58. Alligood, K.T., Yorke, E.D., Yorke, J.A.: Why period-doubling cascades occur: periodic orbit creation followed by stability shedding. *Physica D* **28**, 197–205 (1987). [https://doi.org/10.1016/0167-2789\(87\)90130-8](https://doi.org/10.1016/0167-2789(87)90130-8)
59. Karnatak, R., Kantz, H., Bialonski, S.: Early warning signal for interior crises in excitable systems. *Phys. Rev. E* (2017). <https://doi.org/10.1103/PhysRevE.96.042211>
60. Thompson, J.M.T., Stewart, H.B., Ueda, Y.: Safe, explosive and dangerous bifurcations in dissipative dynamical systems. *Phys. Rev. E* (1994). <https://doi.org/10.1103/PhysRevE.49.1019>
61. Eckmann, J.P.: Roads to turbulence in dissipative dynamical systems. *Rev. Mod. Phys.* **53**, 643–654 (1981). <https://doi.org/10.1103/RevModPhys.53.643>
62. Alligood, K.T., Sauer, T.D., Springer, J.A.Y.: *Chaos: An Introduction to Dynamical Systems*. Springer, New York (1996)
63. Dakos, V., Carpenter, S.R., Nes, E.H., Scheffer, M.: Resilience indicators: prospects and limitations for early warnings of regime shifts. *Philos. Trans. R. Soc. B Biol. Sci.* **370**, 1–10 (2015). <https://doi.org/10.1098/rstb.2013.0263>
64. Nazarimehr, F., Jafari, S., Mohammad, S., Golpayegani, R.H., Perc, M., Sprott, J.C.: Predicting tipping points of dynamical systems during a period-doubling route to chaos. *Chaos* **28**, 73102 (2018). <https://doi.org/10.1063/1.5038801>
65. Moghadam, N.N., Nazarimehr, F., Jafari, S., Sprott, J.C.: Studying the performance of critical slowing down indicators in a biological system with a period-doubling route to chaos. *Phys. A Stat. Mech. Appl.* (2020). <https://doi.org/10.1016/j.physa.2019.123396>
66. Tzuk, O., Ujjwal, S.R., Fernandez-Oto, C., Seifan, M., Meron, E.: Period doubling as an indicator for ecosystem sensitivity to climate extremes. *Sci. Rep.* (2019). <https://doi.org/10.1038/s41598-019-56080-z>
67. Grebogi, C., Ott, E., Yorke, J.A.: Crises, sudden changes in chaotic attractors, and transient chaos. *Physica D* **7**, 181–200 (1983). [https://doi.org/10.1016/0167-2789\(83\)90126-4](https://doi.org/10.1016/0167-2789(83)90126-4)
68. Pomeau, Y., Manneville, P.: Intermittent transition to turbulence in dissipative dynamical systems. *Commun. Math. Phys.* **74**, 189–197 (1980). <https://doi.org/10.1007/BF01197757>
69. Clements, C.F., Ozgul, A.: Including trait-based early warning signals helps predict population collapse. *Nat. Commun.* (2016). <https://doi.org/10.1038/ncomms10984>
70. Carpenter, S.R., Brock, W.A.: Rising variance: a leading indicator of ecological transition. *Ecol. Lett.* **9**, 311–318 (2006). <https://doi.org/10.1111/j.1461-0248.2005.00877.x>
71. Guttal, V., Jayaprakash, C.: Changing skewness: an early warning signal of regime shifts in ecosystems. *Ecol. Lett.* **11**, 450–460 (2008). <https://doi.org/10.1111/j.1461-0248.2008.01160.x>
72. Carpenter, S.R., Brock, W.A., Cole, J.J., Kitchell, J.F., Pace, M.L.: Leading indicators of trophic cascades. *Ecol. Lett.* **11**, 128–138 (2008). <https://doi.org/10.1111/j.1461-0248.2007.01131.x>
73. Dakos, V., Nes, E.H.V., Donangelo, R., Fort, H., Scheffer, M.: Spatial correlation as leading indicator of catastrophic shifts. *Thyroid Res.* **3**, 163–174 (2010). <https://doi.org/10.1007/s12080-009-0060-6>
74. Chen, Z., Li, Y., Liang, H., Yu, J.: Improved permutation entropy for measuring complexity of time series under noisy condition. *Complexity* (2019). <https://doi.org/10.1155/2019/1403829>
75. Guttal, V., Jayaprakash, C.: Spatial variance and spatial skewness: leading indicators of regime shifts in spatial ecological systems. *Thyroid Res.* **2**, 3–12 (2009). <https://doi.org/10.1007/s12080-008-0033-1>
76. Prettyman, J., Livina, V.: Tipping points and early warning signals with applications to geophysical data (2020). <https://doi.org/10.48683/1926.00098364>
77. Dakos, V., Carpenter, S.R., Brock, W.A., Ellison, A.M., Guttal, V.: Methods for detecting early warnings of critical transitions in time series illustrated using simulated ecological data. *PLoS ONE* **7**, 41010 (2012). <https://doi.org/10.1371/journal.pone.0041010>
78. Schultz, P., Menck, P.J., Heitzig, J., Kurths, J.: Potentials and limits to basin stability estimation. *New J. Phys.* (2017). <https://doi.org/10.1088/1367-2630/aa5a7b>
79. Datsieris, G., Wagemakers, A.: Effortless estimation of basins of attraction. *Chaos* (2022). <https://doi.org/10.1063/5.0076568>
80. McDonald, S.W., Grebogi, C., Ott, E., Yorke, J.A.: Fractal basin boundaries. *Physica D* **17**, 125–153 (1985)
81. Borchers, H.W.: *pracma: practical numerical math functions*. R package version 2.4.4 (2023). <https://CRAN.R-project.org/package=pracma>
82. Soetaert, K., Petzoldt, T., Setzer, R.W.: Solving differential equations in R: package deSolve. *J. Stat. Softw.* **33**, 1–25 (2010). <https://doi.org/10.18637/jss.v033.i09>
83. Dessavre, A.G., Southall, E., Tildesley, M.J., Dyson, L.: The problem of detrending when analysing potential indicators of disease elimination. *J. Theor. Biol.* **481**, 183–193 (2019). <https://doi.org/10.1016/j.jtbi.2019.04.011>
84. O'Brien, D.A., Deb, S., Gal, G., Thackeray, S.J., Dutta, P.S., Matsuzaki, S.S., May, L., CF, C.: Early warning signals have limited applicability to empirical lake data. *Nat. Commun.* **14**, 7942 (2023). <https://doi.org/10.1038/s41467-023-43744-8>
85. Boettiger, C., Hastings, A.: Quantifying limits to detection of early warning for critical transitions. *J. R. Soc. Interface* **9**, 2527–2539 (2012). <https://doi.org/10.48550/arxiv.1204.6231>
86. Nahm, F.S.: Receiver operating characteristic curve: overview and practical use for clinicians. *Korean J. Anesthesiol.* **75**, 25 (2022). <https://doi.org/10.4097/KJA.21209>
87. Youden, W.J.: Index for rating diagnostic tests. *Cancer* **3**, 32–35 (1950). <https://doi.org/10.1002/1097->

- 0142(1950)3:1<32::AID-CNCR2820030106>3.0.CO;2-3
88. Team, R.C.: R: a language and environment for statistical computing, Vienna, Austria (2023). <https://www.R-project.org/>
 89. Evers, K.: bifurcationEWS (2023). <https://github.com/KCEvers/bifurcationEWS>
 90. Bury, T.M.: ewstools: a python package for early warning signals of bifurcations in time series data. *J. Open Source Softw.* **8**, 5038 (2023)
 91. Boxtel, G.V.: gsignal: Signal processing (2021). <https://github.com/gjmvanboxtel/gsignal>
 92. Livina, V.N., Lenton, T.M.: A modified method for detecting incipient bifurcations in a dynamical system. *Geophys. Res. Lett.* (2007). <https://doi.org/10.1029/2006GL028672>
 93. Wijnants, M.L., Cox, R.F.A., Hasselman, F., Bosman, A.M.T., Orden, G.V.: Does sample rate introduce an artifact in spectral analysis of continuous processes? *Front. Physiol.* (2013). <https://doi.org/10.3389/fphys.2012.00495>
 94. Boerlijst, M.C., Oudman, T., Roos, A.M.D.: Catastrophic collapse can occur without early warning: examples of silent catastrophes in structured ecological models. *PLoS ONE* (2013). <https://doi.org/10.1371/journal.pone.0062033>
 95. Patterson, A.C., Strang, A.G., Abbott, K.C.: When and where we can expect to see early warning signals in multi-species systems approaching tipping points: insights from theory. *Am. Nat.* **198**, 12–26 (2021). <https://doi.org/10.1086/714275>
 96. Grziwotz, F., Chang, C.W., Dakos, V., Nes, E.H., Schwarzländer, M., Kamps, O., Heßler, M., Tokuda, I.T., Telschow, A., Hsieh, C.H.: Anticipating the occurrence and type of critical transitions: supplementary. *Sci. Adv.* (2023). <https://doi.org/10.1126/sciadv.abq4558>
 97. Ali, F., Menzinger, M.: On the local stability of limit cycles. *Chaos* **9**, 348–356 (1999). <https://doi.org/10.1063/1.166412>
 98. Kurrer, C., Schulten, K.: Effect of noise and perturbations on limit cycle systems. *Physica D* **50**, 311–320 (1991). [https://doi.org/10.1016/0167-2789\(91\)90001-P](https://doi.org/10.1016/0167-2789(91)90001-P)
 99. Weinans, E., Quax, R., Nes, E.H., Leemput, I.A.: Evaluating the performance of multivariate indicators of resilience loss. *Sci. Rep.* (2021). <https://doi.org/10.1038/s41598-021-87839-y>
 100. Pavithran, I., Unni, V.R., Sujith, R.I.: Critical transitions and their early warning signals in thermoacoustic systems. *Eur. Phys. J. Spec. Top.* **230**, 3411–3432 (2021). <https://doi.org/10.1140/epjs/s11734-021-00214-w>
 101. Kleinen, T., Held, H., Petschel-Held, G.: The potential role of spectral properties in detecting thresholds in the earth system: application to the thermohaline circulation. *Ocean Dyn.* **53**, 53–63 (2003). <https://doi.org/10.1007/s10236-002-0023-6>
 102. Prettyman, J., Kuna, T., Livina, V.: A novel scaling indicator of early warning signals helps anticipate tropical cyclones. *Europhys. Lett.* (2018). <https://doi.org/10.1209/0295-5075/121/10002>
 103. George, S.V., Kachhara, S., Ambika, G.: Early warning signals for critical transitions in complex systems. *Phys. Scr.* (2021). <https://doi.org/10.1088/1402-4896/acde20>
 104. Grebogi, C., Ott, E., Yorke, J.A.: Critical exponent of chaotic transients in nonlinear dynamical systems. *Phys. Rev. Lett.* **57**, 1284–1287 (1986). <https://doi.org/10.1103/PhysRevLett.57.1284>
 105. Blume, S.O.P., Sansavini, G.: Effects of stressor characteristics on early warning signs of critical transitions and “critical coupling” in complex dynamical systems. *Chaos* (2017). <https://doi.org/10.1063/1.5008315>
 106. Williamson, M.S., Bathiany, S., Lenton, T.M.: Early warning signals of tipping points in periodically forced systems. *Earth Syst. Dyn.* **7**, 313–326 (2016). <https://doi.org/10.5194/esd-7-313-2016>
 107. O’Regan, S.M., Burton, D.L.: How stochasticity influences leading indicators of critical transitions. *Bull. Math. Biol.* **80**, 1630–1654 (2018). <https://doi.org/10.1007/s11538-018-0429-z>
 108. Carpenter, S.R., Brock, W.A.: Early warnings of unknown nonlinear shifts: a nonparametric approach. *Ecology* **92**, 2196–2201 (2011). <https://doi.org/10.1890/11-0716.1>
 109. Dakos, V., Scheffer, M., Nes, E.H.V., Brovkin, V., Petoukhov, V., Held, H.: Slowing down as an early warning signal for abrupt climate change. *Proc. Natl. Acad. Sci. U.S.A.* **105**, 14308–14312 (2008). <https://doi.org/10.1073/pnas.0802430105>
 110. Drake, J.M., Griffen, B.D.: Early warning signals of extinction in deteriorating environments. *Nature* **467**, 456–459 (2010). <https://doi.org/10.1038/nature09389>
 111. Harris, M.J., Hay, S.I., Drake, J.M.: Early warning signals of malaria resurgence in Kericho, Kenya. *Biol. Lett.* (2020). <https://doi.org/10.1098/rsbl.2019.0713>
 112. Rogers, B.M., Solvik, K., Hogg, E.H., Ju, J., Masek, J.G., Michaelian, M., Berner, L.T., Goetz, S.J.: Detecting early warning signals of tree mortality in boreal North America using multiscale satellite data. *Glob. Change Biol.* **24**, 2284–2304 (2018). <https://doi.org/10.1111/gcb.14107>
 113. Veraart, A.J., Faassen, E.J., Dakos, V., Nes, E.H.V., Lüring, M., Scheffer, M.: Recovery rates reflect distance to a tipping point in a living system. *Nature* **481**, 357–359 (2012). <https://doi.org/10.1038/nature10723>
 114. Lenton, T.M., Livina, V.N., Dakos, V., Nes, E.H.V., Scheffer, M.: Early warning of climate tipping points from critical slowing down: comparing methods to improve robustness. *Trans. R. Soc. A* **370**, 1185–1204 (2012). <https://doi.org/10.1098/rsta.2011.0304>
 115. Pace, M.L., Carpenter, S.R., Johnson, R.A., Kurtzweil, J.T.: Zooplankton provide early warnings of a regime shift in a whole lake manipulation. *Limnol. Oceanogr.* **58**, 525–532 (2013). <https://doi.org/10.4319/lo.2013.58.2.0525>
 116. Cline, T.J., Seekell, D.A., Carpenter, S.R., Pace, M.L., Hodgson, J.R., Kitchell, J.F., Weidel, B.C.: Early warnings of regime shifts: evaluation of spatial indicators from a whole-ecosystem experiment. *Ecosphere* (2014). <https://doi.org/10.1890/ES13-00398.1>
 117. Snippe, E., Smit, A.C., Kuppens, P., Burger, H., Ceulemans, E.: Recurrence of depression can be foreseen by monitoring mental states with statistical process control. *J. Psychopathol. Clin. Sci.* **132**, 145–155 (2023). <https://doi.org/10.1037/abn0000812>
 118. Burthe, S.J., Henrys, P.A., Mackay, E.B., Spears, B.M., Campbell, R., Carvalho, L., Dudley, B., Gunn, I.D.M., Johns, D.G., Maberly, S.C., May, L., Newell, M.A., Wan-

- less, S., Winfield, I.J., Thackeray, S.J., Daunt, F.: Do early warning indicators consistently predict nonlinear change in long-term ecological data? *J. Appl. Ecol.* **53**, 666–676 (2016). <https://doi.org/10.1111/1365-2664.12519>
119. Boettner, C., Klinghammer, G., Boers, N., Westerhold, T., Marwan, N.: Early-warning signals for Cenozoic climate transitions. *Quat. Sci. Rev.* (2021). <https://doi.org/10.1016/j.quascirev.2021.107177>
 120. Bos, F.M., Schreuder, M.J., George, S.V., Doornbos, B., Bruggeman, R., Kriek, L., Haarman, B.C.M., Wichers, M., Snippe, E.: Anticipating manic and depressive transitions in patients with bipolar disorder using early warning signals. *Int. J. Bipolar Disord.* (2022). <https://doi.org/10.1186/s40345-022-00258-4>
 121. Helmich, M.A., Smit, A.C., Bringmann, L.F., Schreuder, M.J., Oldehinkel, A.J., Wichers, M., Snippe, E.: Detecting impending symptom transitions using early-warning signals in individuals receiving treatment for depression. *Clin. Psychol. Sci.* **11**, 994–1010 (2023). <https://doi.org/10.1177/21677026221137006>
 122. Ditlevsen, P.D., Johnsen, S.J.: Tipping points: early warning and wishful thinking. *Geophys. Res. Lett.* (2010). <https://doi.org/10.1029/2010GL044486>
 123. Clements, C.F., Drake, J.M., Griffiths, J.L., Ozgul, A.: Factors influencing the detectability of early warning signals of population collapse. *Am. Nat.* **186**, 50–58 (2015). <https://doi.org/10.1086/681573>
 124. Gsell, A.S., Scharfenberger, U., Özkundakci, D., Walters, A., Hansson, L.A., Janssen, A.B.G., Nöges, P., Reid, P.C., Schindler, D.E., Donk, E.V., Dakos, V., Adrian, R.: Evaluating early-warning indicators of critical transitions in natural aquatic ecosystems. *Proc. Natl. Acad. Sci. U.S.A.* **113**, 8089–8095 (2016). <https://doi.org/10.1073/pnas.1608242113>
 125. Arkilanian, A.A., Clements, C.F., Ozgul, A., Baruah, G.: Effect of time series length and resolution on abundance- and trait-based early warning signals of population declines. *Ecology* (2020). <https://doi.org/10.1002/ecy.3040>
 126. Perretti, C.T., Munch, S.B.: Regime shift indicators fail under noise levels commonly observed in ecological systems. *Ecol. Appl.* **22**, 1772–1779 (2012). <https://doi.org/10.1890/11-0161.1>
 127. Dai, L., Korolev, K.S., Gore, J.: Relation between stability and resilience determines the performance of early warning signals under different environmental drivers. *Proc. Natl. Acad. Sci.* **112**, 10056–10061 (2015). <https://doi.org/10.5061/dryad.k30v3>
 128. Dablander, F., Heesterbeek, H., Borsboom, D., Drake, J.M.: Overlapping timescales obscure early warning signals of the second Covid-19 wave. *Proc. R. Soc. B Biol. Sci.* (2022). <https://doi.org/10.1098/rspb.2021.1809>
 129. Proverbio, D., Kemp, F., Magni, S., Gonçalves, J.: Performance of early warning signals for disease re-emergence: a case study on Covid-19 data. *PLoS Comput. Biol.* (2022). <https://doi.org/10.1371/journal.pcbi.1009958>
 130. Boettiger, C., Hastings, A.: Early warning signals and the prosecutor's fallacy. *Proc. R. Soc. B Biol. Sci.* **279**, 4734–4739 (2012). <https://doi.org/10.1098/rspb.2012.2085>
 131. Singh, B.K., Parham, P.E., Hu, C.K.: Structural perturbations to population skeletons: transient dynamics, coexistence of attractors and the rarity of chaos. *PLoS ONE* (2011). <https://doi.org/10.1371/journal.pone.0024200>
 132. Clements, C.F., Ozgul, A.: Indicators of transitions in biological systems. *Ecol. Lett.* **21**, 905–919 (2018). <https://doi.org/10.1111/ele.12948>
 133. Grziwotz, F., Chang, C.-W., Dakos, V., Nes, E.H., Schwarzländer, M., Kamps, O., Heßler, M., Tokuda, I.T., Telschow, A., Hsieh, C.: Anticipating the occurrence and type of critical transitions. *Sci. Adv.* (2023). <https://doi.org/10.1126/sciadv.abq4558>
 134. Litzow, M.A., Hunsicker, M.E.: Early warning signals, nonlinearity, and signs of hysteresis in real ecosystems. *Ecosphere* (2016). <https://doi.org/10.1002/ecs2.1614>
 135. Bestelmeyer, B.T., Ellison, A.M., Fraser, W.R., Gorman, K.B., Holbrook, S.J., Laney, C.M., Ohman, M.D., Peters, D.P.C., Pillsbury, F.C., Rassweiler, A., Schmitt, R.J., Sharma, S.: Analysis of abrupt transitions in ecological systems. *Ecosphere* **2**, 129 (2011). <https://doi.org/10.1890/es11-00216.1>
 136. Clements, C.F., Mccarthy, M.A., Blanchard, J.L.: Early warning signals of recovery in complex systems. *Nat. Commun.* (2019). <https://doi.org/10.1038/s41467-019-09684-y>
 137. Mann, H.B.: Nonparametric tests against trend. *Econometrica* **13**, 245–259 (1945)
 138. Montgomery, D.C.: *Introduction to Statistical Quality Control*. Wiley, New York (2009)
 139. Schat, E., Tuerlinckx, F., Smit, A.C., Ketelaere, B., Ceulemans, E.: Detecting mean changes in experience sampling data in real time: a comparison of univariate and multivariate statistical process control methods. *Psychol. Methods* **28**, 1335–1357 (2021). <https://doi.org/10.1037/MET0000447>
 140. Bury, T.M., Sujith, R.I., Pavithran, I., Scheffer, M., Lenton, T.M., Anand, M., Bauch, C.T.: Deep learning for early warning signals of tipping points. *Proc. Natl. Acad. Sci. U.S.A.* **118**, 2106140118 (2021). https://doi.org/10.1073/PNAS.2106140118/SUPPL_FILE/PNAS.2106140118.SAPP.PDF
 141. Bury, T.M., Dylewsky, D., Bauch, C.T., Anand, M., Glass, L., Shrier, A., Bub, G.: Predicting discrete-time bifurcations with deep learning. *Nat. Commun.* (2023). <https://doi.org/10.1038/s41467-023-42020-z>

Publisher's Note Springer Nature remains neutral with regard to jurisdictional claims in published maps and institutional affiliations.